Performance and Oscillatory Behavior of PBI-Phosphoric Acid based Higher-Temperature Vapor Feed Direct Methanol Fuel Cells

Master's Thesis

Submitted to the faculty of

Chemical Engineering Department

Worcester Polytechnic Institute,

Worcester, MA 01609

April 29, 2015

By:

Yan Dong

Approved by:

_____

Prof. Ravindra Datta, Advisor

_____

Prof. David DiBiasio, Department Head

Abstract

Operation of a Direct Methanol Fuel Cell (DMFC) at high temperature with vapor feed can avoid many of the issues of conventional low temperatures DMFC, such as crossover, low efficiency and high catalyst loading. Here we investigate the behavior of a PBI-phosphoric acid membrane based DMFC. This project has two goals. The first goal is to investigate the effect of temperature and methanol concentration on the performance of Direct Methanol Fuel Cell (DMFC). The second goal is to investigate the effect of temperature and methanol on its oscillatory behavior under constant current or constant voltage operation. In this project, we use a commercial polybenzimidazole (PBI)-phosphoric acid based membrane electrode assembly (MEA), namely, Celtec-P 1100 from BASF. The Celtec-P 1100 MEA is actually designed for high temperature operation with referenced hydrogen. This kind of MEA operates at temperatures between 140℃ to 180℃, tolerating high concentrations of carbon monoxide and running independently of humidification. This study uses different vaporized concentration methanol instead of hydrogen at the anode and oxygen at the cathode. We tested in different conditions, the concentration of methanol from 1M to 10M and the operating temperature from 160℃ to 180℃. Results show that the performance of fuel cell increases with temperature up to 180℃ and the effect of methanol concentration is small. Further, oscillatory behavior is observed and reported for the first time. The oscillation is not significantly affected by the temperature and methanol concentration, current density or voltage. However, the oscillation is in special region in different condition.

Acknowledgements

There are many individuals that I would like to acknowledge for their help and contribution to this project and the fuel cell laboratory.

First, William Lind, Sean Callaghan and Matthew Suarez who conducted on the research about high temperature direct methanol fuel cell. Second, I would like to thank Susan Yen and Drew Martino who also work in fuel cell laboratory. Finally, I would like to thank Professor Ravindra Datta for allowing me to work in his laboratory, and for his invaluable guidance. I am very grateful to have this opportunity to work for him. This experience is invaluable in my future study and work.

Contents

Figure list

Chapter 1: Introduction

The global energy consumption increased from about 283 quadrillion Btu in 1980 to 508 quadrillion Btu in 2010 (U.S. Energy Information Administration). Most of this energy comes from fossil fuels, such as oil, coal and nature gas. However, this has some issues. One is that fossil fuels are limit and so the price of fossil fuels is increasing. The other is that the fossil fuels emit greenhouse gas CO_2 during combustion along with other pollutants. For these reasons, research on new energy efficient methods to generate energy and sustainable fuels is becoming more and more important, such as solar energy, wind, biomass and hydrogen. Fuel cell technology is one of the promising technologies. Fuel cells can be used in many fields. First, they can be used in large-scale power generation, which is more efficient and environmentally-friendly than the conventional thermal power plants. Second, fuel cells can be used for on-site emergency power supply, such as in a hospital and control point. Third, fuel cell powered vehicles appear promising. Fourth, they can be used as small power supply for personal computer or cell phone (Bagotsky, 2012).

Fuel cells have been known of for a long time. William Grove discovered the fundamental principle of fuel cells by reversing water electrolysis to generate electricity from hydrogen and oxygen. A fuel cell is an electrochemical “device” that continuously converts chemical energy into electric energy (and some heat) for as long as fuel and oxidant are supplied (Hoogers, 2003). A basic fuel cell system is made of the components, shown in Figure 1, which it also shows how it works: hydrogen flows through the bipolar plate channels on the anode side and hydrogen passes through the gas diffusion layer (GDL). Hydrogen is then oxidized on the anode catalyst and the

protons pass through the polymer electrolyte membrane (PEM) to the cathode side while electrons proceed to the outer circuit where useful work is extracted from them. Oxygen from air flows through the channels on the cathode side, passes through the gas diffusion layer and is reduced on the cathode catalyst layer by the protons arriving via the PEM and electrons from the external circuit. During this process, the fuel cell produces electrical energy (Debe, 2012). By stacking fuel cells (Figure 1), any desired voltage and current may be obtained.

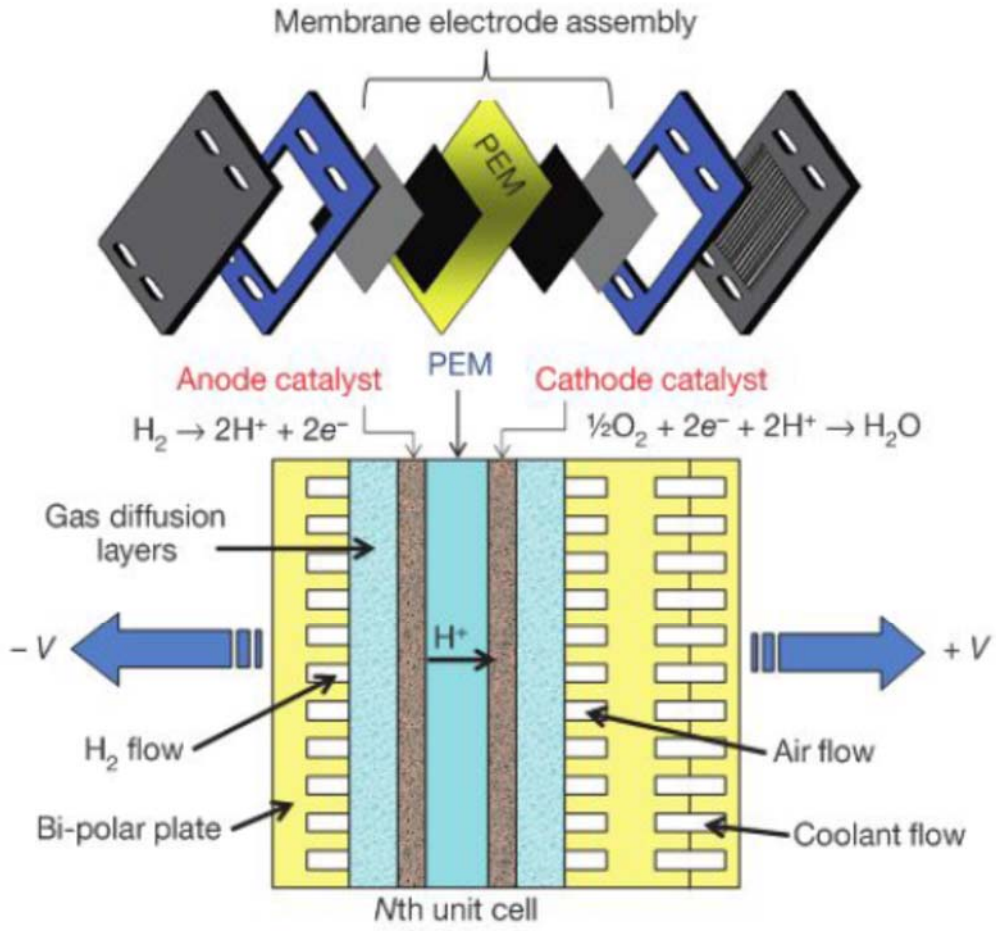

Figure 1. Fuel cell components (Debe, 2012).

A key distinction between fuel cells and batteries is that battery cannot produce energy. Batteries just store electoral energy and release it (Sedighizaheh and Rezazadeh, 2007). Fuel cells

as the other hand, are like an energy “factory”, producing electricity (O’Hayre et al, 2006.). Based on the operating temperature of fuel cells, fuel cells may be divided in two main groups, the low temperature and the high temperature fuel cells. Low temperature (<100℃) fuel cells include Alkaline Fuel Cells (AFC), Proton Exchange Membrane Fuel Cells (PEMFC) and the Direct Methanol Fuel Cells (DMFC). Fuel cells which can operate at 500 – 1000℃ are the high temperature fuel cells. High temperature fuel cells are two different types, the Solid Oxide Fuel Cell (SOFC) and the Molten Carbonate Fuel Cell (MCFC) (Carrette et al, 2000). In the intermediate temperature ranges (200-500℃), there are no practical fuel cells, except the phosphoric acid fuel cell (PAFC) that operates around 180℃. If fuel cells be developed in this ranges, they would have several advantages including lower cast catalysts.

Direct methanol fuel cell (DMFC) is one of the special type of low temperature fuel cells, which uses methanol as a fuel. Compared with hydrogen, methanol has some advantages. Because methanol is liquid, it is easy to store and transport in most climate conditions. It has a high energy density (about 1.8 kWh kg^{-1} or 1.7kWh L^{-1}), it is easy to store and is much cheaper than hydrogen. For the DMFC, since we do not need to convert methanol to hydrogen, so it can be used in many application including road transportation (McNicol et al, 1999), on-site portable energy and emergency back-up energy, e.g. for hospitals. Direct Methanol fuel cell is one of the special forms of PEM fuel, based on Nafion and polybenzimidazole (PBI)-based membrane cells (Carrette et al, 2000). The Nafion-based membrane only works effectively at temperatures under 100℃. At temperatures above 100℃, the water in the membrane is evaporated, which reduces the proton transport leading to low performance of the membranes. PBI-based membranes can work at higher temperatures up to 180℃.

There are two issues with the conventional Nafion-based direct methanol fuel cells (DMFC). The first is anode catalyst poisoning. When methanol is adsorbed on the catalyst to be converted to protons and electrons, there are some intermediate products formed in the reaction networks. One of them is carbon monoxide (CO), which strongly adsorbs on the catalyst covering the surface and reducing kinetics. Under 100 ℃, it is difficult to desorb. It thus causes a significant decrease in performance and requires a large amount of previous metal catalyst. The other issue is methanol crossover from the anode side to the cathode side, which causes depolarization losses at the cathode along with fuel and efficiency losses. Methanol crossover increases with the increase of methanol concentration, increase of temperature and decrease of the membrane thickness (Heinzel and Barrgan, 1999). As a result, practical DMFC feeds are very dilute, usually 1 M methanol or less.

In this project, I use PBI-based membrane for a vapor feed direct methanol fuel cell (DMFC). Compared with Nafion-based membranes, PBI-based membranes can work at higher temperatures (160-180℃). At these temperatures, CO can partly be desorbed from the catalysts, which reduces the catalyst poisoning, reduces catalyst coating, allow concentrated feeds and increase the performance of the fuel cell systems. Further, kinetics of the reaction are also higher at high temperatures. Furthermore, PBI-based membranes have a lower methanol crossover by one order of magnitude than Nafion (Wang et al, 1996). Vaporized methanol, instead of liquid as fuel, was used and the experiment was run at temperatures from 160℃ to 180℃ to test the performance under different conditions of temperature and methanol concentration. During the experiment works, it was noted that there are oscillations at constant current scan and also at constant voltage scan. There are further discussed in this report.

In Chapter two, the background of fuel cell, all components in fuel cell systems, and system issues are discussed. My methodology is described in Chapter three. Chapter four is about the results and discussion of the research. The conclusions and recommendations are discussed in Chapter five.

Chapter 2: Literature Review

2.1 History of Direct Methanol Fuel Cells

Methanol can be prepared via three methods: 1) from fossil-fuel-based syn-gas, 2) via methane oxidation, and 3) via carbon dioxide reduction with hydrogen (Olah, 2005), as is shown in Figure 2.

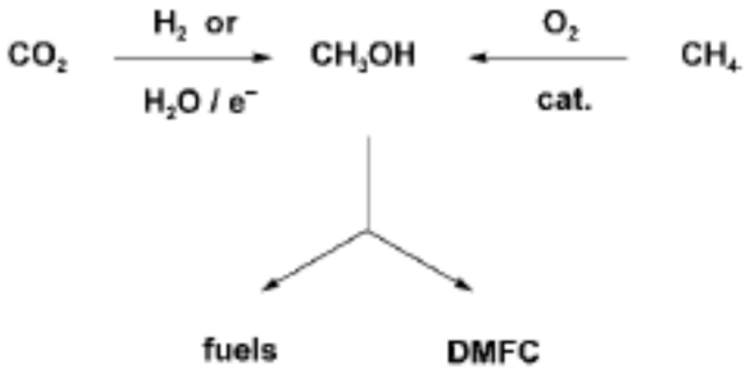

Figure 2. Three methods to prepare methanol (Olah, 2005).

From Figure 2, it is shown that hydrogen can be stored as methanol, a convenient liquid, which is easy to store and transport. Methanol also has a high energy density, which is shown in Table 1 and Figure 3. Ethanol has a higher energy density, but it is much more difficult to cleave C-C bonds than C-H bonds. Thus, methanol is a more practical fuel than ethanol in fuel cells.

Table 1. Volumetric and gravimetric energy density for various fuels for low temperature fuel cells (Arico et al, 2009).

Fuels	Volumetric Energy density ($kWh\,l^{-1}$)	Gravimetric Energy density ($kWh\,kg^{-1}$)
Diluted Hydrogen (1.5%)	—	0.49
Hydrogen	0.18 (@ 1000 psi, 25 °C)	—
Methanol	4.82 (100 wt.%)	6.1
Ethanol	6.28 (100 wt.%)	8
Formic acid	1.75 (88 wt.%)	—
Dimethyl ether (DME)	5.61 (in liquid of 100 wt.%)	8.4
Ethylene glycol	5.87 (100 wt.%)	5.3

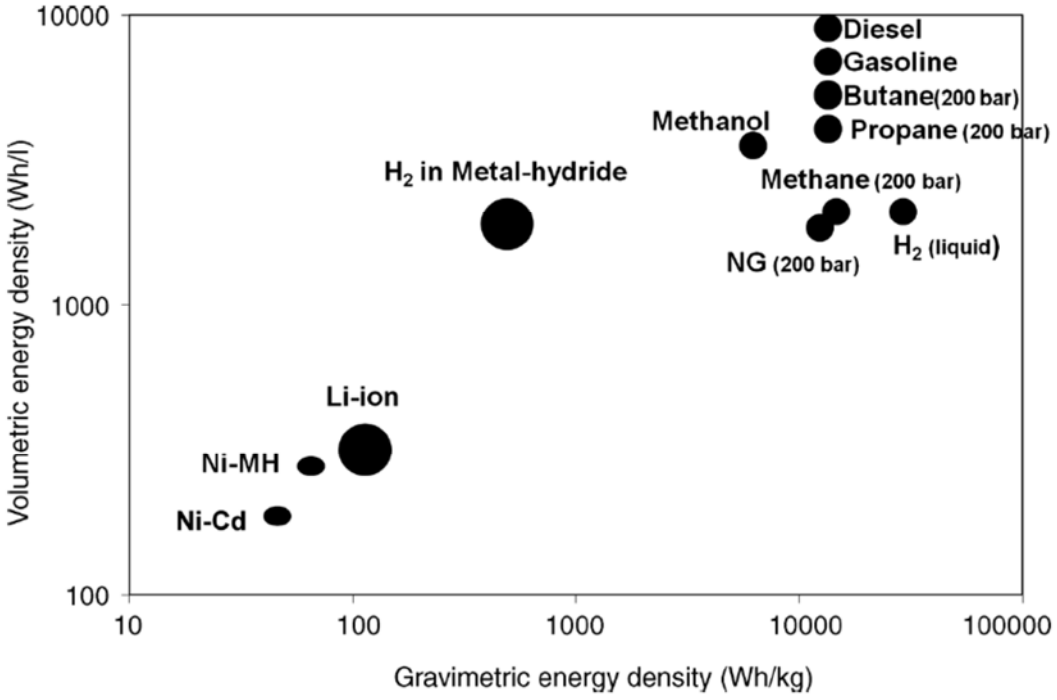

Figure 3. Gravimetric and volumetric energy density of various fuels/ devices (Arico et al, 2009).

Research in direct methanol fuel cells has a long history. E. Muller was the first person to explore the methanol electro-oxidation in 1922 (Arico et al, 2009). Kordesch, Marko and Pavela began to investigate methanol fuel cells in the early 1950s. (Arico et al, 2009). Alkaline electrolytes were initially used in methanol fuel cells. However, the main problem is that liquid alkaline electrolytes, such as KOH, can react with the CO_2, which is produced during methanol

oxidation. Research on DMFCs was also focused on the search for active anode formulations, because that the methanol oxidation was even slower than the oxygen reduction on the cathode side. Thus, half-cell studies were popular at that time (Arico et al, 2009).

The investigation of DMFCs in polymer electrolyte single cells replaced the half-cell studies in liquid electrolytes in the 1990s, which was a new era for DMFCs. Another significant progress was that the study of combinatorial catalysts suggested that multifunctional catalysts will make a big difference in performance (Arico et al, 2009).

2.2 Overview of Direct Methanol Fuel Cell (DMFC)

Conventional DMFCs use the PEM technology. Thus, they have the same structure as H_2-O_2 PEMFCs. Figure 4 shows the structure of a single of direct methanol fuel cell. There are three important parts: anode, polymer electrolyte membrane and cathode. For anode and cathode, each side consist of Gas Diffusion Layer (GDL) and a catalyst layer. Gas diffusion layers are a porous material, which are always made from a dense array of carbon fibers. Gas diffusion layers play an important role in:1) fuel diffusion, 2) CO_2 gas removal, 3) diffusion of water, 4) effective heat transfer during cell operation. The catalyst layer is the place where the reduction and oxidation reaction happens. The polymer electrolyte membrane is typically on Nafion.

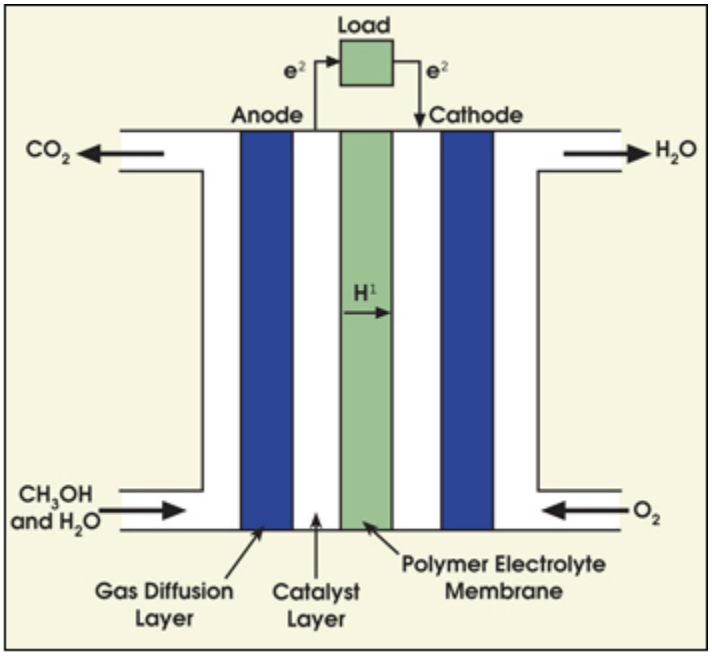

Figure 4. Direct Methanol Fuel Cell (Savage, 2008).

TO operate DFMCs, we pump liquid methanol solution to the anode side. Methanol molecules diffuse through the gas diffusion layer to the catalyst layer, where they adsorb on the catalyst and react to form protons and electrons, releasing carbon dioxide. Electrons are collected externally energy. The protons pass through the PEM to the cathode and react with oxygen, and with depleted energy state electrons from the external circuit, to produce water. The anode, cathode and the overall reactions for DMFCs are:

$$Anode: CH_3OH + H_2O \rightarrow CO_2 + 6H^+ + 6e^- (1)$$

$$Cathode: 1.5O_2 + 6H^+ + 6e^- \rightarrow 3H_2O (2)$$

$$Overall: CH_3OH + 1.5O_2 \rightarrow 2H_2O + CO_2 (3)$$

The thermodynamic parameters of the overall reaction are:

The enthalpy of the reaction: $\Delta H_{OR}^{O} = -726 \frac{kJ}{mol} = 1.25\ eV$

The Gibbs reaction energy of the reaction: $\Delta G_{OR}^{O} = -702 \frac{kJ}{mol} = 1.21\ eV$

2.2.1 Anode

The anode of a DMFC consists of a gas diffusion layer (GDL) and a catalyst layer. The GDL is made from carbon fiber, and performs the following functions: 1) reactants and products can diffuse through, 2) it must be thermally and electrically conductive, 3) the pores of the side facing catalyst layer must be small to prevent the catalyst going through the GDL, 4) it must be rigid enough to support the MEA (Sammes, 2006). Catalyst layer is crucial part in the anode where reacting occur, so most research on the anode is on the catalyst layer. One key issue in DMFCs is the slow anode kinetics. Often other metals are added to improve the performance of Pt. Many metals have been found to have a positive effect on methanol oxidation, such as Re, Ru, Os, Rh, Mo, Pb, Bi and Sn (Carrette et al, 2000). However, the most active catalyst is Pt-Ru. The function of Ruthenium (Ru) is to lower the overpotential at the anode, by activing water at lower potential, so that it can reduce the poisoning and increase the catalytic of the pure platinum (Baldauf, and Preidel, 1999). The methanol electrosorption and reaction at Pt catalyst are shown in Figure, leading to CO adsorption.

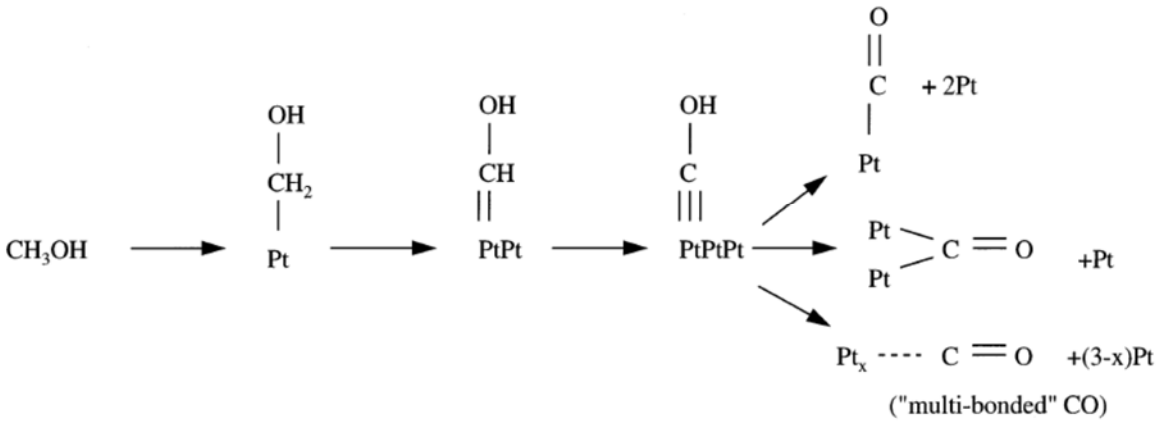

Figure 5. Scheme of the consecutive dissociative electrosorption of methanol at Pt (Wasmus, and Kuver, 1998).

The reaction steps on the Pt are believed to take place though a sequence of steps as (Hamnett, 1997):

$$CH_3OH + Pt(s) \rightarrow Pt - CH_2OH + H^+ + e^- (4)$$
$$Pt - CH_2OH + Pt(s) \rightarrow Pt_2 - CHOH + H^+ + e^- (5)$$
$$Pt_2CH_2OH + Pt(s) \rightarrow Pt_3 - COH + H^+ + e^- (6)$$
$$Pt_3COH \rightarrow Pt - CO + 2Pt(s) + H^+ + e^- (7)$$
$$Pt(s) + H_2O \rightarrow Pt - OH + H^+ + e^- (8)$$
$$PtOH + Pt \rightarrow Pt - COOH (9a)$$

Or

$$Pt - CO + H_2O \rightarrow Pt - COOH + H^+ + e^- (9b)$$
$$Pt - COOH \rightarrow Pt(s) + CO_2H^+ + e^- (10)$$

Additional reactions that also have been suggested include:

$$Pt - CH_2OH \rightarrow Pt(s) + HCHO + H^+ + e^- (11)$$
$$Pt_2CHOH + Pt - OH \rightarrow 3Pt(s) + HCOOH + H^+ + e^- (12)$$

Or

$$Pt\ CHOH + H_2O \rightarrow 2Pt(s) + HCOOCH + 2H^+ + e^- (13)$$
$$Pt_3 + Pt - OH \rightarrow 3Pt(s) + Pt - COOH + H^+ + e^- (14)$$

Or

$$Pt_3C-OH+H_2O \rightarrow 2Pt(s)+Pt-COOH+2H^+ +2e^- (15)$$

2.2.2 Cathode

The cathode of the DMFCs also consists of two parts: 1) a carbon fiber GDL, and 2) a catalyst layer typically Pt. It uses the same GDL as the anode. However, the catalyst layer is different from the anode. The research on the cathode catalyst has two orientations (Li et al, 2004). One is due to the methanol crossover, with some researches trying to find methanol tolerant catalysts such as metal phthalocynines, porphyrins, metal oxides, metal carbides and ruthenium-based chalcogenides (Reeve et al, 2000, Reeve et al, 1998). The other is based on Pt and the alloys with other transitional metals, such as Pt-Co, Pt-Cr, Pt/Ni and Pt-Fe (Shukla et al, 2001 and Mukerjee et al, 1995). The oxygen reduction reaction (ORR) on the cathode is:

$$Cathode: 1.5O_2+6H^+ +6e^- \rightarrow 3H_2O(2)$$

The oxygen reduction reaction steps on the cathode catalyst are (Arisetty et al, 2010):

$$Pt+O_2+H^+ +e^- \rightarrow PtO_2H(16)$$
$$PtO_2H+3H^+ +3e^- \leftrightarrow Pt+2H_2O(17)$$

Compared with the kinetics of the anode side, the cathode side is somewhat faster. Thus, most research about the DMFC catalysts are on the anode side.

2.2.3 Membrane

The DMFCs have the same MEA structure as the PEMFCs. The heart of DMFCs and PEMFCs are the polymer membrane which has some unique characters: 1) relatively high proton conductivity, 2) impermeable to gases and other fuels, 3) stable in fuel cell systems (Gottesfeld and Zawodzinski, 1997). The membrane is placed between the anode and the cathode. The catalyst layer is at the interface of the membrane, as shown in Figure 6.

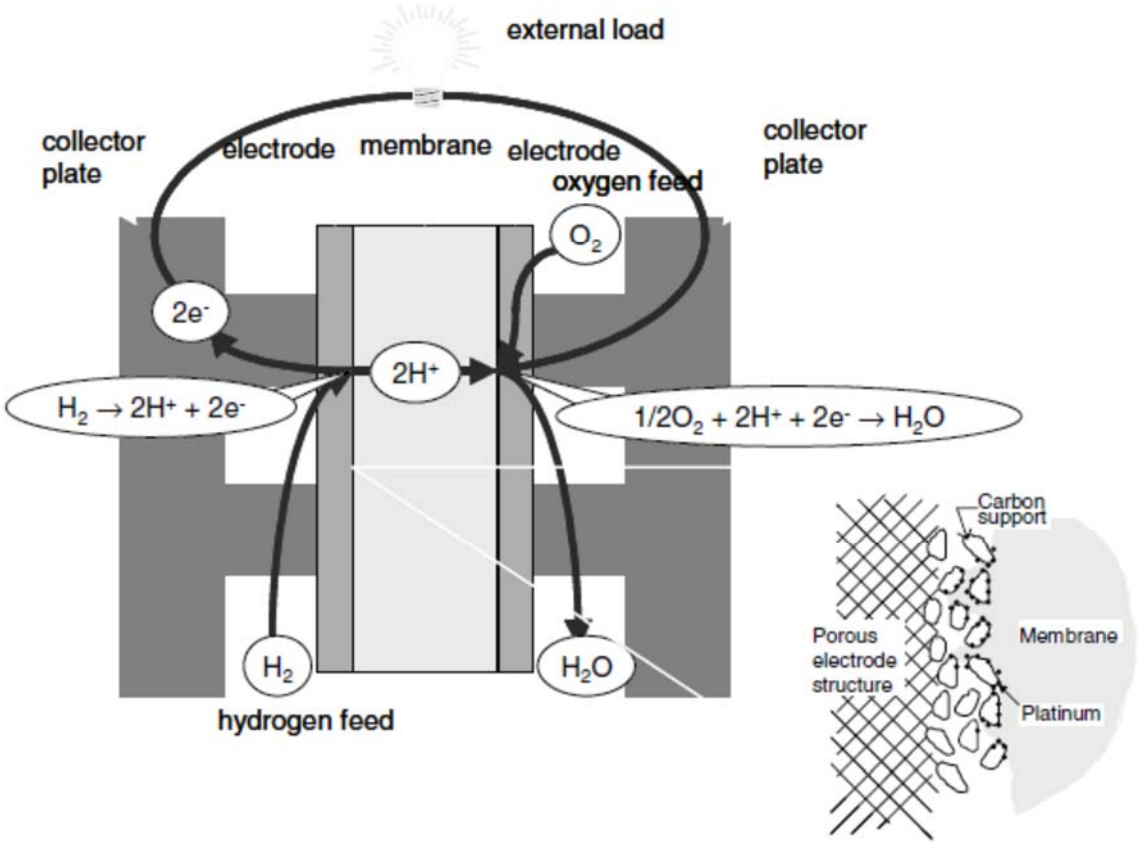

Figure 6. Polymer membrane in fuel cell (Barbir, 1997 and Barbir, 2005).

The materials of membrane for the fuel cells should have some unique characters, such as low electron conductivity, high proton conductivity, low permeability to fuel and oxidant, low

water permeability and mechanically or chemically stable. At Ppresent there are two different kinds of common polymer membranes: 1) sulfonated tetrafluoroethylene based fluoropolymer-copolymer, typically called Nafion and manufactured by DuPant, 2) polybenzimidazole (PBI)-Phosphoric acid membrane.

2.2.3.1 Nafion

Nafion was discovered and developed by Walther Grot of DuPont in the late 1960s (DuPont Fuel cell). The structure of Nafion is shown in Figure 7.

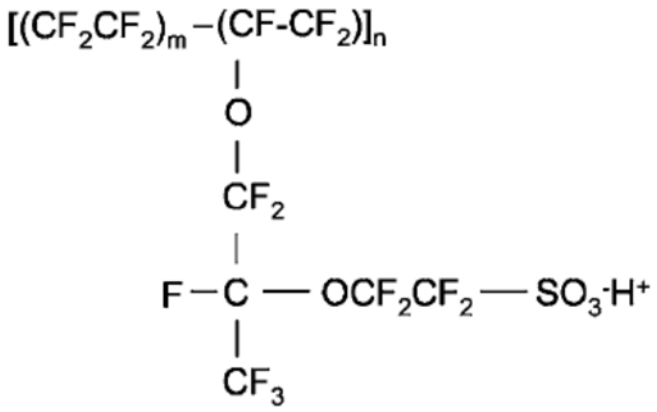

Figure 7. Unit molecular structure for a DuPont Nafion electrolyte (Zhou et al, 2007).

Nafion is synthetized by the copolymerization of tetrafluoroethylene (TFE) and a derivative of a perfluoro with sulfonylacid fluoride (Connoll et al, 1966). Figure 8 shows how Nafion is produced.

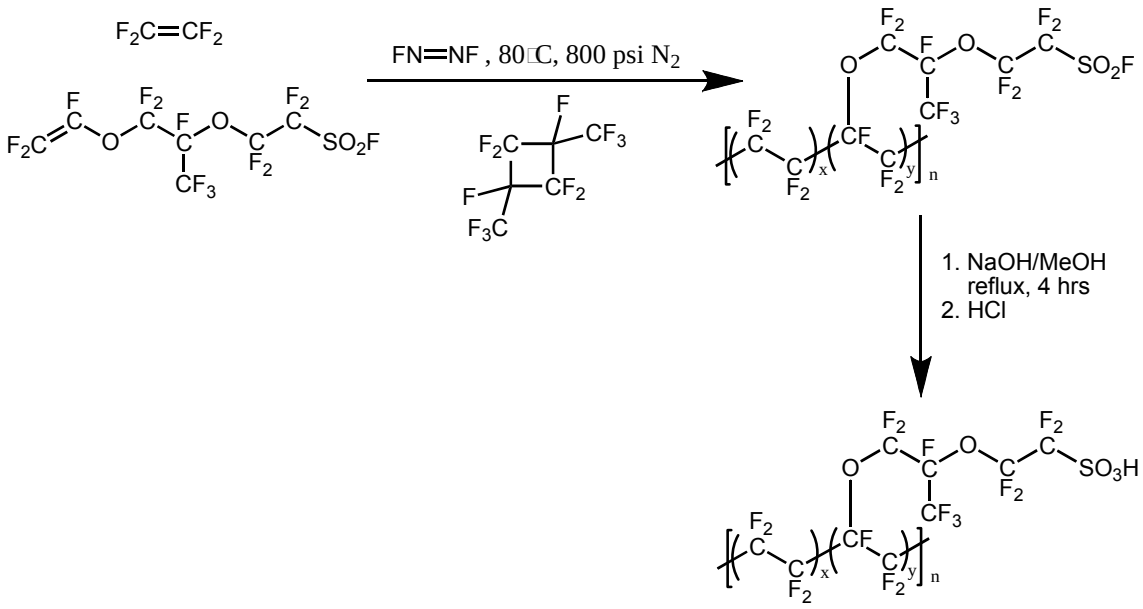

Figure 8. Synthesis of Nafion (Connolly et al, 1966).

Nafion has a number of advantages. It is a stable material with selective ion permeability. It also has high proton conductivity under aqueous conditions due to Teflon backbone of about 0.1 S/cm (Schmidt-Rour and Chen, 2008). From Figure 7, we can see that the PTFE backbone is hydrophobic. On the other hand the sulfonic acid group is strongly hydrophilic. Thus, when water comes into Nafion membrane, it can form aqueous reverse micelles or clusters, which are shown in Figure 9. The protons and the water molecules present are shown by ball-and-stick structure (Voth, 2006). This cluster-network model was first proposed by Gierke and Hsu (Gierke et al, 1982), as shown in Figure 10.

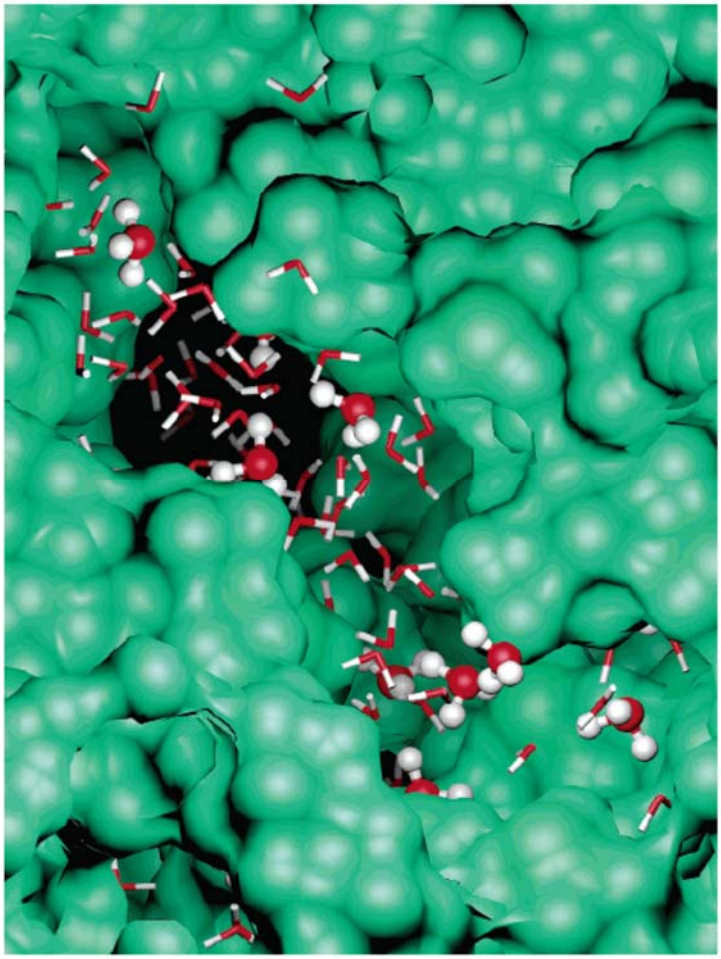

Figure 9. Nafion membrane in hydrated state (Voth., 2006).

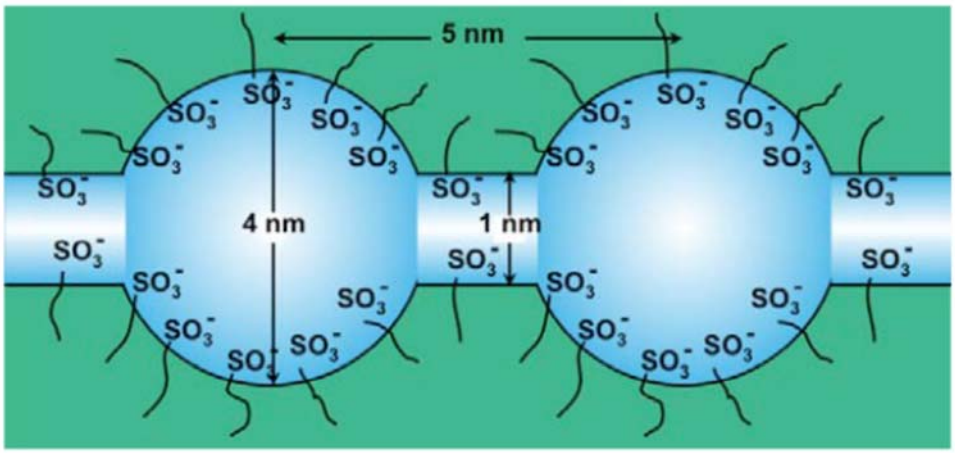

Figure 10. Clusters-network structure of hydrated Nafion (Gierke et al, 1982).

The mechanisms of proton diffusion in Nafion include “vehicle” mechanism and transfer mechanism ((Kreuer, K. et al, 1982)), also called Grotthuss mechanism (Datta, 2014). “Vehicle” mechanism has three steps. First, the proton will form a complex ion with the vehicle molecule, in this case the vehicle molecule is water. Second, the vehicle molecule diffuses and takes the proton diffusion through the membrane which, follows the Nernst-Einstein relation. Third, the vehicle molecule releases proton on other side of the membrane and returns back to the original side. This process is shown in Figure 11.

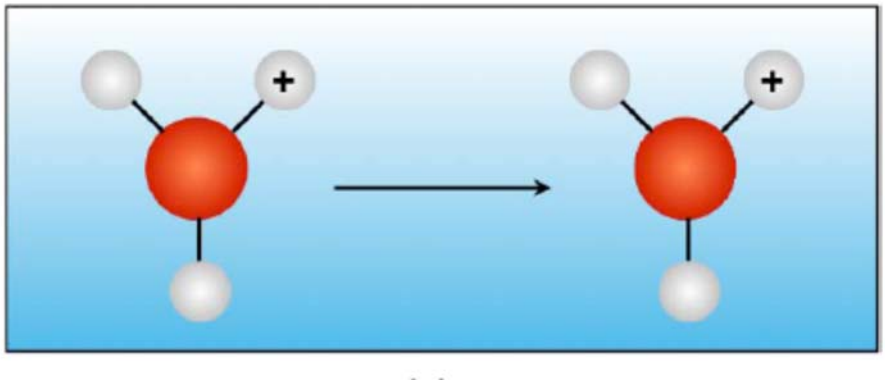

Figure 11. "Vehicle" mechanism (Datta, 2014).

The transfer mechanism, or Grotthuss mechanism, is that the vehicle molecule maintains the same position. The protons transport by the rotation of the vehicle molecule. The process has three steps. First, proton from complex ions with vehicle molecular. Second, vehicle molecule rotates and passes proton to next molecule. Then the proton will be passed by vehicle molecule one by one until it reaches to the other side of the membrane. This mechanism is shown schematically in Figure 12.

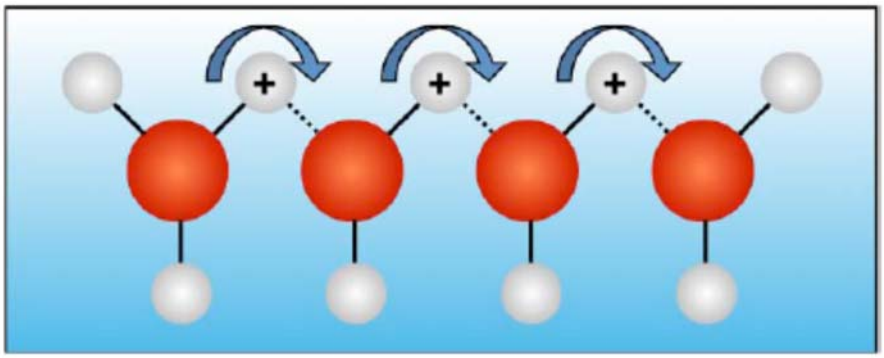

Figure 12. Transfer mechanism or Grotthuss mechanism (Datta, 2014).

Nafion also has some disadvantages. The vehicle molecule is water. Thus, the conductivity drops severely at low water content. Further, it means Nafion cannot work above 100℃, because of water evaporation. In DMFCs, furthermore, Nafion is permeable to methanol and the mechanical strength is poor at higher temperatures.

2.2.3.2 PBI

Polybenzimidazole(PBI) is short for poly[2,2'-(m-phenylen)-5,5'-bisbenzimidazole], which is a polymer with a very high melting point, thermal and chemical stability. It was discovered by Carl Shipp Marvel in the 1950s (Leonard, 1994).The structure of polybenzimidazole is shown in Figure 13.

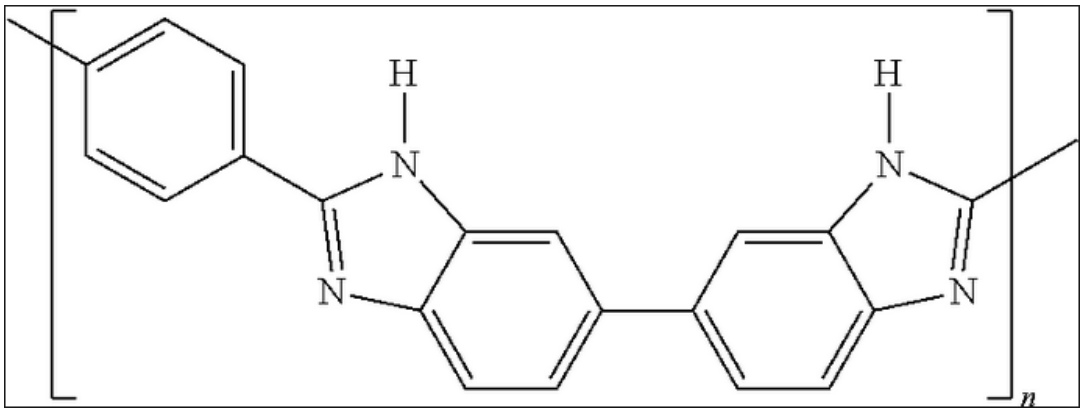

Figure 13. Structure of PBI (Wu, 2013).

Because of these special characteristics, PBI is a good support material for electrolyte such as phosphoric acid for fuel cell membrane. Compared with Nafion-based membrane, PBI-based MEAs have other advantages. The first one is high resistance to fuel impurities, because carbon monoxide can desorb from the catalyst at higher temperature. The second is fast electrode kinetics due to the high temperature. The third is simplified water and thermal management, also because of higher temperature and no need water as a vehicle molecule. In fact, liquid water can leach out the $H_3PO_4^-$ (Vielstich et al, 2009). The fourth advantage, this is that the vapor phase methanol can also decrease the methanol crossover. PBI can be synthetized via the scheme showing in figure 14. The next step is to immerse PBI membrane into aqueous phosphoric acid or sulfuric acid solution to produce acid-doped PBI membrane which can be used in fuel cell. Celtec-P is a commercial membrane, based on polybenzimidazole (PBI) and phosphoric acid, and is made by BASF. This membrane is hygroscopic. Because only two units of phosphoric acid in the membrane can chemically combine with each repeating unit of PBI, most of the supported phosphoric acid is present as “free acid” (Suarez, 2013). Any contact with liquid, this may cause loss of electrolyte. The Celtec-P has a platinum-alloy cathode and a platinum anode, which the catalysts loading is for H_2 and O_2 fuel cells systems (BASF Chemical Company, 2012).

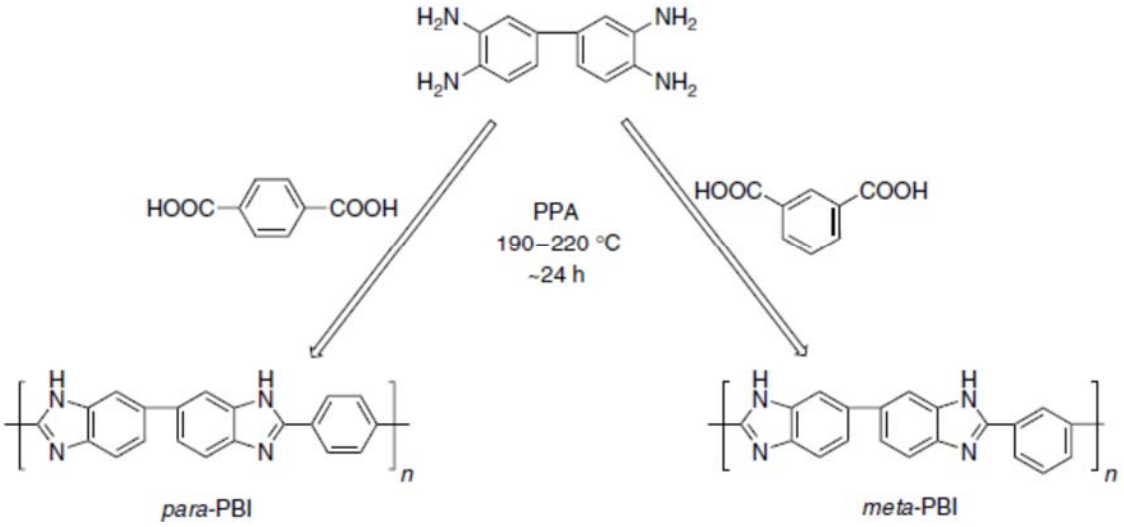

Figure 14. General synthetic scheme for PBI (Vielstich et al, 2009).

2.2.4 Issues with Conventional Direct Methanol Fuel Cells

2.2.4.1 Methanol crossover

Methanol crossover is a big issue for direct methanol fuel cells. The fuel of DMFCs is methanol mixed with water. Thus methanol will readily crossover to the cathode side across the PEM which has water in this process (Larminie and Dicks, 2003). Methanol crossover causes the waste of fuel. In addition, it causes methanol reacting on the cathode catalyst, which will reduce oxygen adsorption and reduction. It reduces the cell voltage (Song et al, 2004). There are many factors which effect methanol crossover, such as membrane structure and morphology, membrane thickness, temperature, pressure and methanol feed concentration (Ahmed and Dincer, 2011). The relation between temperature and feed concentration with on crossover current is shown in Figure 15.

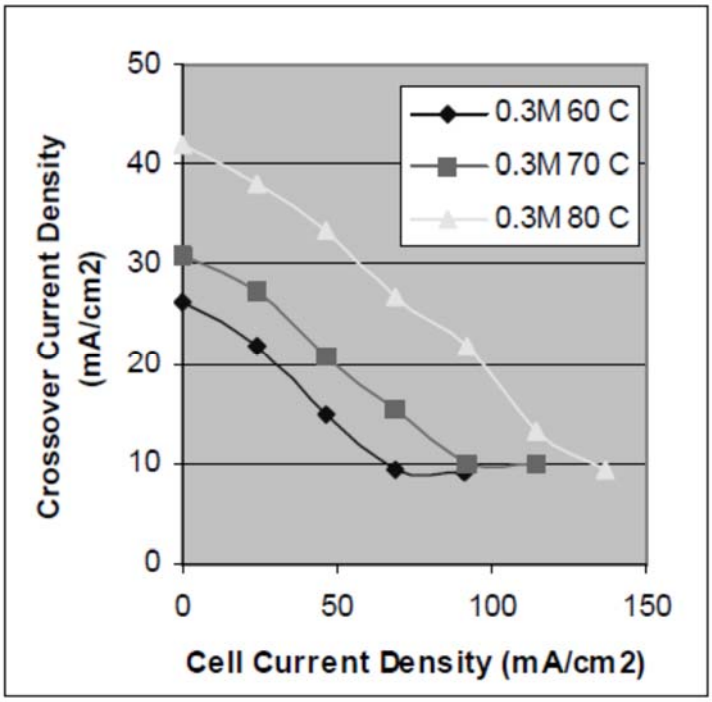

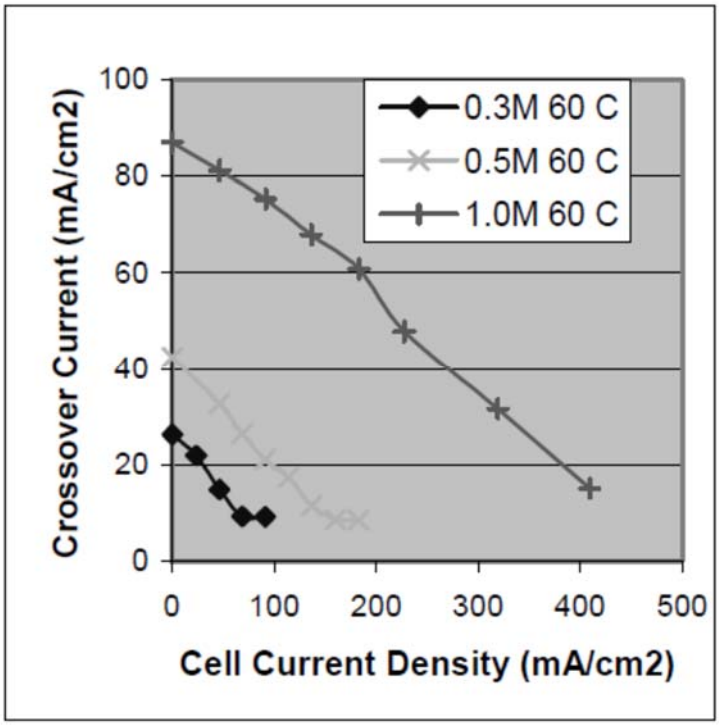

Figure 15.The relation between temperature and methanol concentration (Pivovar et al, 2003).

From Figure 15, we can find that higher temperature and higher methanol concentration will increase methanol crossover.

2.2.4.2 Catalyst poison

The molecule that makes anode catalyst poisoned is carbon monoxide (CO). CO is one of the trace components in hydrogen fuel, and is also an intermediate product of methanol decomposition and oxidation in DMFCs (Waszczuk et al, 2001). Because of the strong affinity CO, it can strongly adsorb on the surface of Pt catalyst and block the active sites (Yan et al, 2008), as shown schematically in Figure 16. Thus, the performance of the catalyst is substantially reduced.

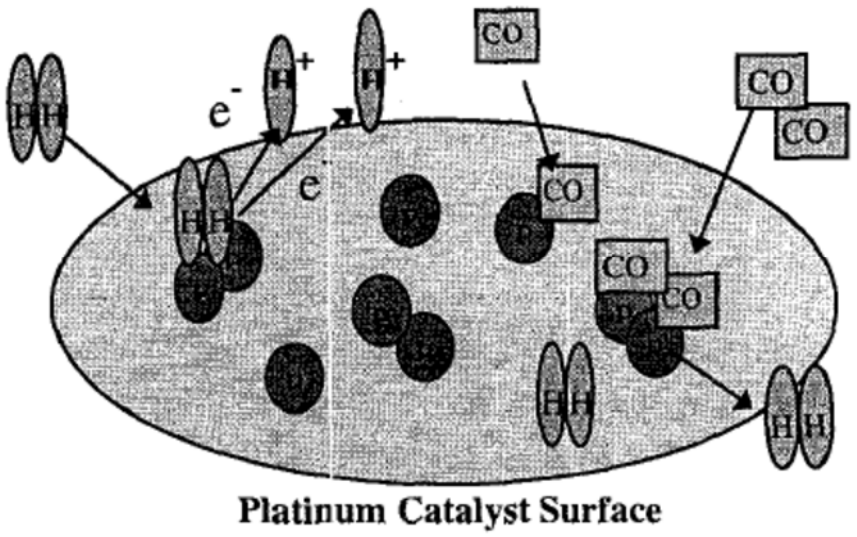

Figure 16 .A schematic of thee CO adsorption on the platinum catalyst (Rodrigues et al, 1997).

There are a couple approaches to combat CO poisoning. One method is to use platinum-alloy anode catalyst, such as ruthenium. Another way is to operate the fuel cell at higher temperature such as 120℃, at which temperature CO can desorb from the catalyst (Yan et al, 2008). During experiments, which the temperatures are above 160℃, I found there are

oscillations in the potential when run at constant current. There are also oscillations in the current, when run at constant voltage. Sustained potential oscillations were also observed by Zhang and Datta in their experiments (Zhang and Datta, 2002). They observed the oscillatory behavior of H_2 and CO mixture, and test the oscillations at different anode flow rates, current densities and temperatures. From their experiment, it is shown that temperature is the most critical factor of the oscillations. Compared with my experiment, the oscillatory behavior maybe cause by the CO adsorption reaction cycle, which will be discussed in results and discussion section.

2.2.5 Typical DMFC performance

2.2.5.1 Nafion Based DMFC

For a conventional Nafion based MEA, as shown in Figure 17, the overall performance increased with the increasing of fuel cell temperature (Chen and Yang, 2003). They also Chen and Yang also showed a comparison of methanol concentration to fuel cell performance. The peak power density was compared in different methanol concentrations, such as 0.5, 1.5, 3.0, 6.0, 9.0 wt%, as shown in Figure 18. We can see that the performance increases until the methanol concentration reaches 3.0 wt%. The power density decreases as the methanol concentration increase from 3.0 to 9.0 wt% (Chen and Yang, 2003)

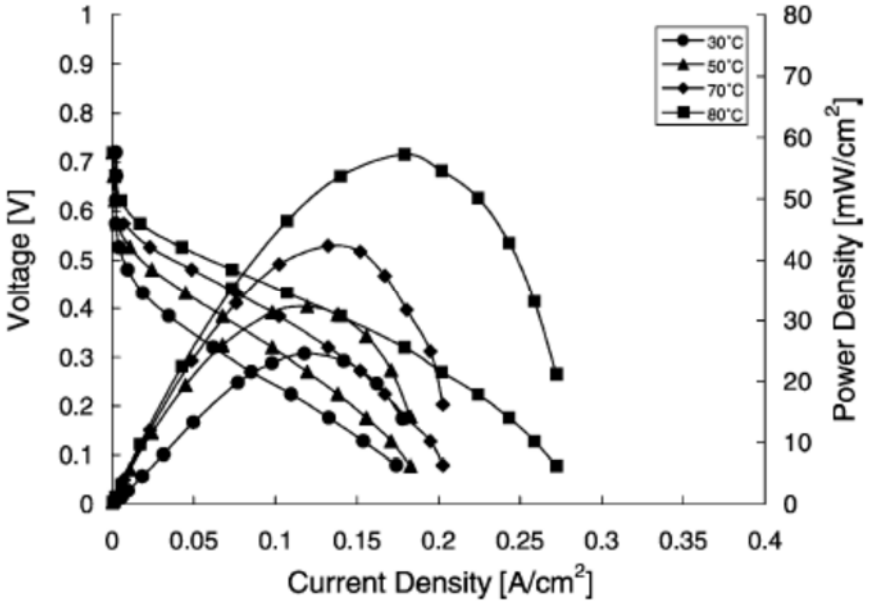

Figure 17. Performance of air-breathing DMFC at various methanol solution temperatures with 3 wt% MeOH (Chen and Yang, 2003).

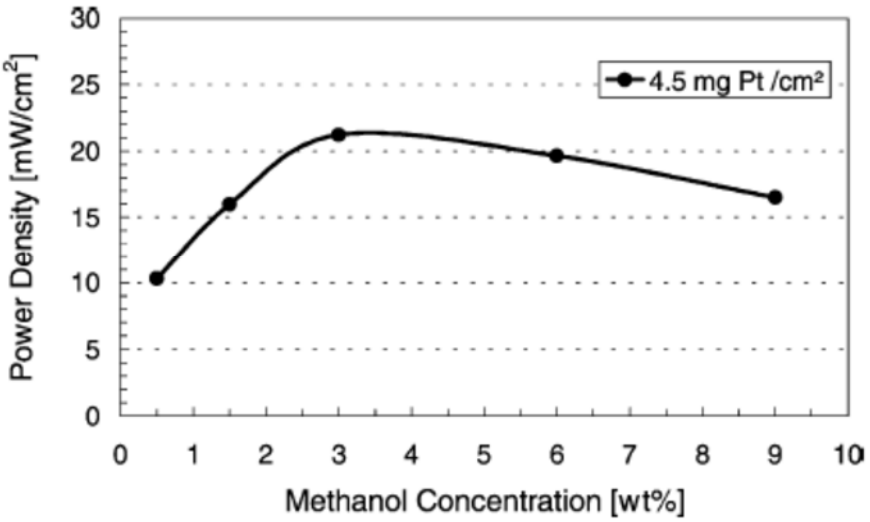

Figure 18. Variation of power density with methanol concentration at 30 ℃（Chen and Yang, 2003).

2.2.5.2 PBI-Phosphoric acid DMFC

In 1995, Wainright et al. reported PBI-based fuel cell used in a DMFC system for the first time (Wang et al, 1996). PBI-Phosphoric acid based membrane has several advantages, such as work in higher temperature and low methanol crossover. The influence of temperature on the cell performance is shown in Figure 19. Figure 19 shows that the performance increases as the increasing of temperature, which can be explained by the enhancement of the electrode kinetics and the decrease on the membrane resistance (Lobato et al, 2008).

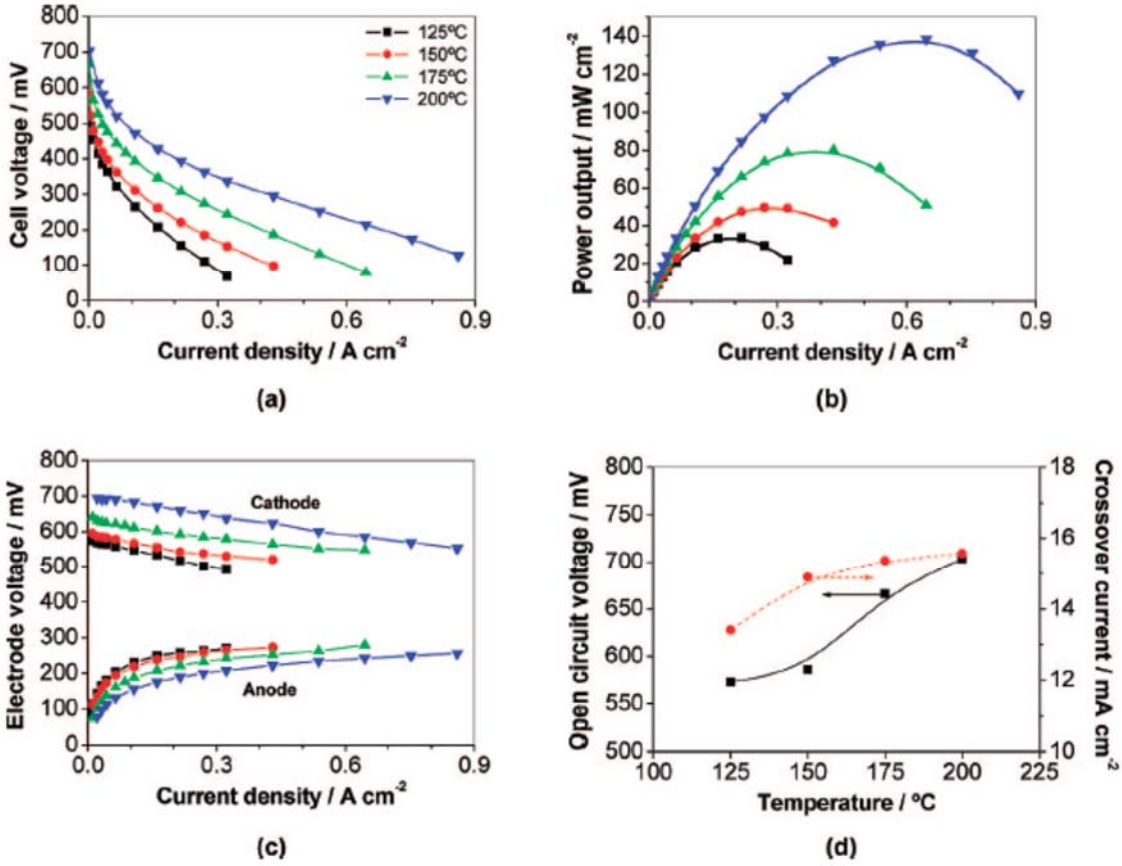

Figure 19. Influence of the temperature on the cell performance of a vapor-fed PBI-based DMFC (M/W=0.5; cathode= pure O2; no backpressure) (a) Cell voltage, (b) power output, (c) electrode overvoltage, and (d) open circuit voltage and methanol crossover current (Lobato et al, 2008)

The influence of methanol concentration on the cell performance is shown in Figure 20. Figure 20 shows that the cell performance increase as the methanol concentration increase from M/W=0.25 to M/W= 0.5, and will decrease as M/W=0.5 to M/W=2, which because at high methanol concentration the methanol crossover increases (Lobato et al, 2008).

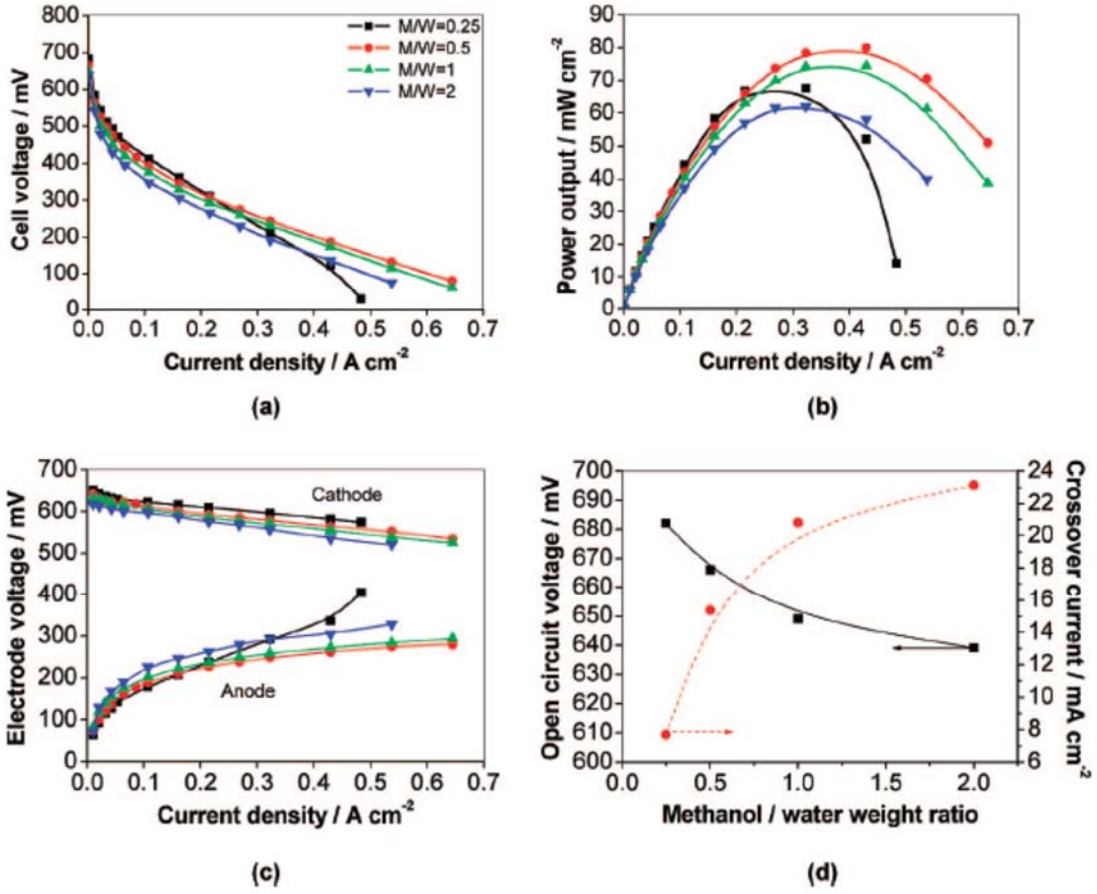

Figure 20. Influence of the methanol/water weight ratio on the cell performance of vapor-fed PBI-based DMFC (T=175C; cathode=pure O2); no backpressure). (a) Cell voltage, (b) power output, (c) electrode overvoltage, and (d) open circuit voltage and methanol crossover density (Lobato et al, 2008)

Chapter 3: Methodology

In this works, I test the performance of PBI-phosphoric acid DMFC at different concentrations and temperatures. The test methanol concentrations are 1 mol/L, 3 mol/L, 5 mol/L, 7.5 molL and 10 mol/L. The temperatures vary from 160℃ to 180℃. At the same time, I also ran the constant current scan as well as constant voltage scan at different methanol concentrations and temperatures to observe the oscillations, caused presumably by the cycle of CO adsorption and recovered on the surface. The fuel cell test station is shown schematically in Figure 21.

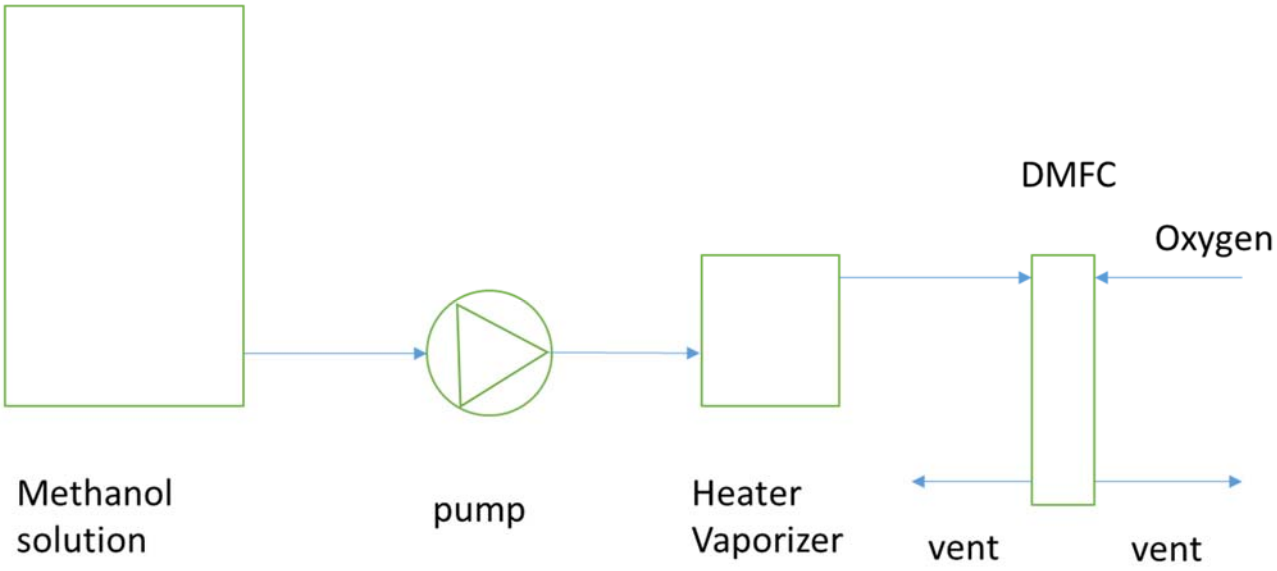

Figure 21. Schematic description of the DMFC system.

The experimental procedure is that the methanol and water mixture go into the pump (ISCO, Model 1000D). Then the pump compresses the solution into the heater. The solution will

be heated to the temperature which we want and vapor to the vapored methanol solution. The vapored phase methanol go into the anode side and the oxygen go into the cathode side. The deta ils of the apparatus will be discussed in Appendix B.

The membrane that I use is Celtec-P 1100 from BASF Chemical Company. Celtec-P 1100 is a commercial PBI-PA Membrane Electrode Assembllies (MEA), which can works at temperature from 120 to 180℃ and it is high tolerance to impurities. The surface area of this MEA is 50 cm^2 and are square, which means that each side is about 7.1 cm. The active area of the membrane is 45 cm^2. It has a platinum-alloy cathode platinum anode. The membrane thickness is about 850 microns. The membrane shows in Figure 22. There is a cut corner on one side of the membrane which indicates the cathode.

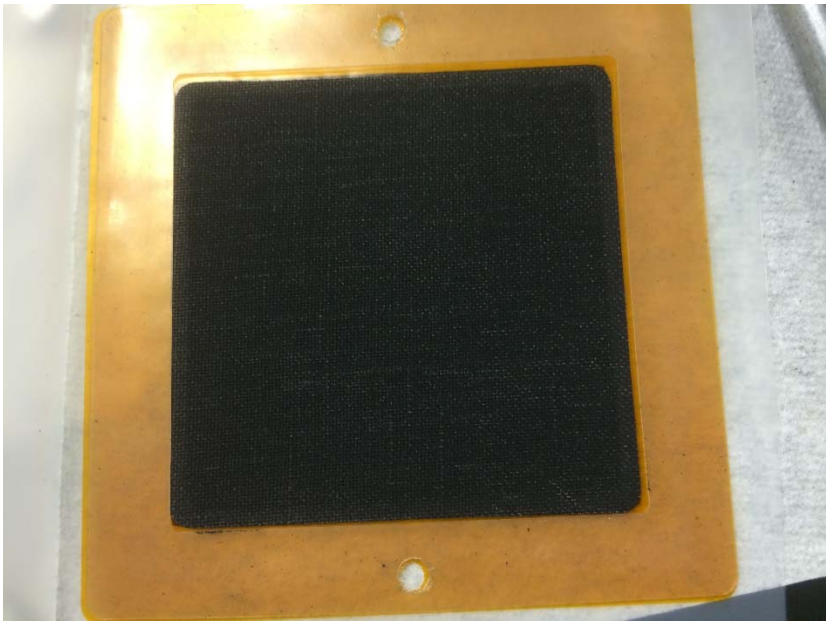

Figure 22. MEA.

3.1 Apparatus

3.1.1 Single test cell for high temperature Celtec-P MEAs

The structure of the test cell for Celtec-P 1100 is shown in figure 23.

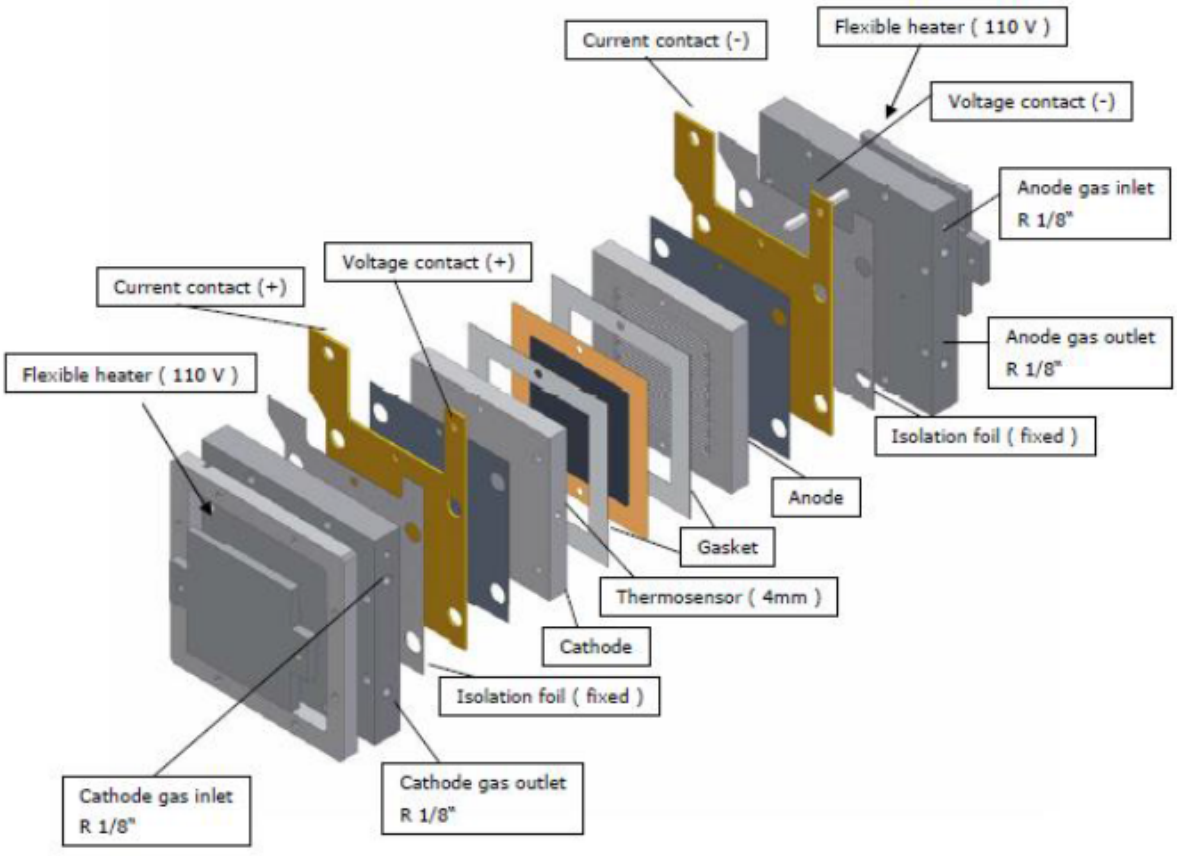

Figure 23. structure of single test fuel cell (BASF Chemical Company).

As seen, there are many components. First from the left is the flexible heater, which can heat the fuel cell to the temperature we want. Second is the graphite block for the fuel cell with

cathode gas inlet and cathode gas outlet. Third is isolation foil, which is to insulate the current collector from the support. Fourth is the current collector, which is in contact with the load box. Thus, we can control voltage or current to test fuel cell by the load box and get feedback. Fifth is the cathode, with channels for oxygen in it. The structure is then repeated on the anode part of the fuel cell. Figure 24 is a picture of the assembly single test fuel cell.

Figure 24. Picture of single test fuel cell.

From Figure 24, we can see that the feed lines connect at the top, and waste lines connect at the bottom. A thermocouple is inserted into the cathode to help monitor and control the fuel cell temperature.

3.1.2 Fuel cell test station

The overall fuel cell test station is shown in Figure 25.

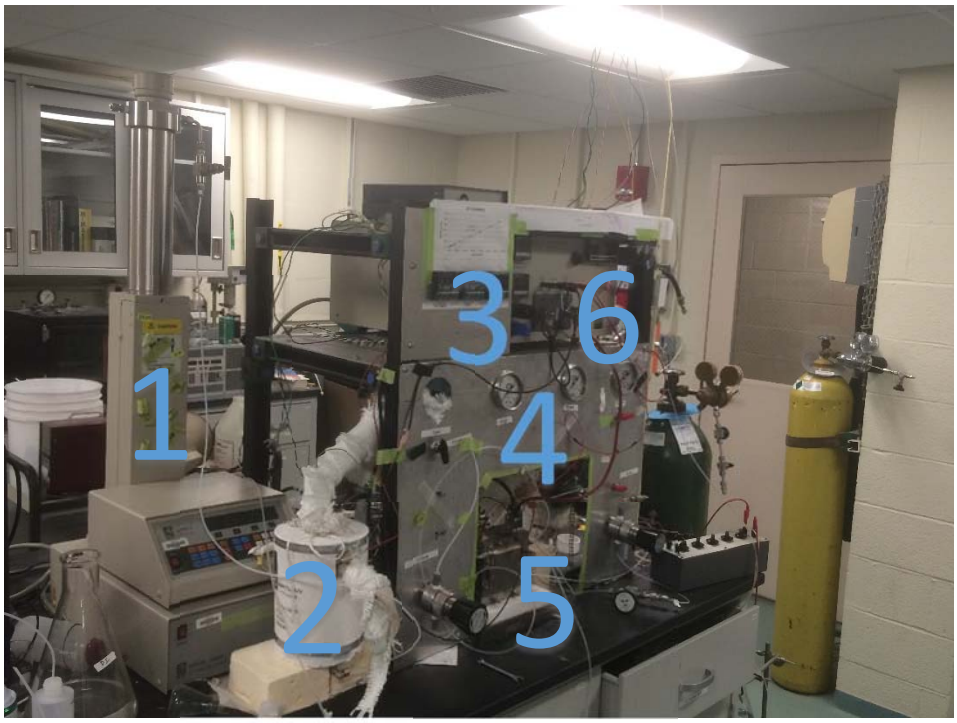

Figure 25. Fuel cell test station.

In Figure 25, methanol-water mixed solution is stored in syringe pump (1). Syringe pump pumps the solution into the vaporing furnace (2). Methanol-water mixed solution is heated and becomes vapor phase methanol in the furnace. Then vapor phase methanol goes into anode of fuel cell (5). Oxygen goes into cathode of fuel cell (5). Temperature controller (3) is used to control the temperatures of furnace, fuel cell, and the methanol feed line. Load box (6) which connects with computer can be used to input voltage or current as we need and monitor the corresponding electrical output.

3.2 Activation of PBI-Based MEA

Before test, it is important to make sure the MEA is in the best state. Thus we need to activate it. First, as per the prescribed procedure, with H_2/O_2.

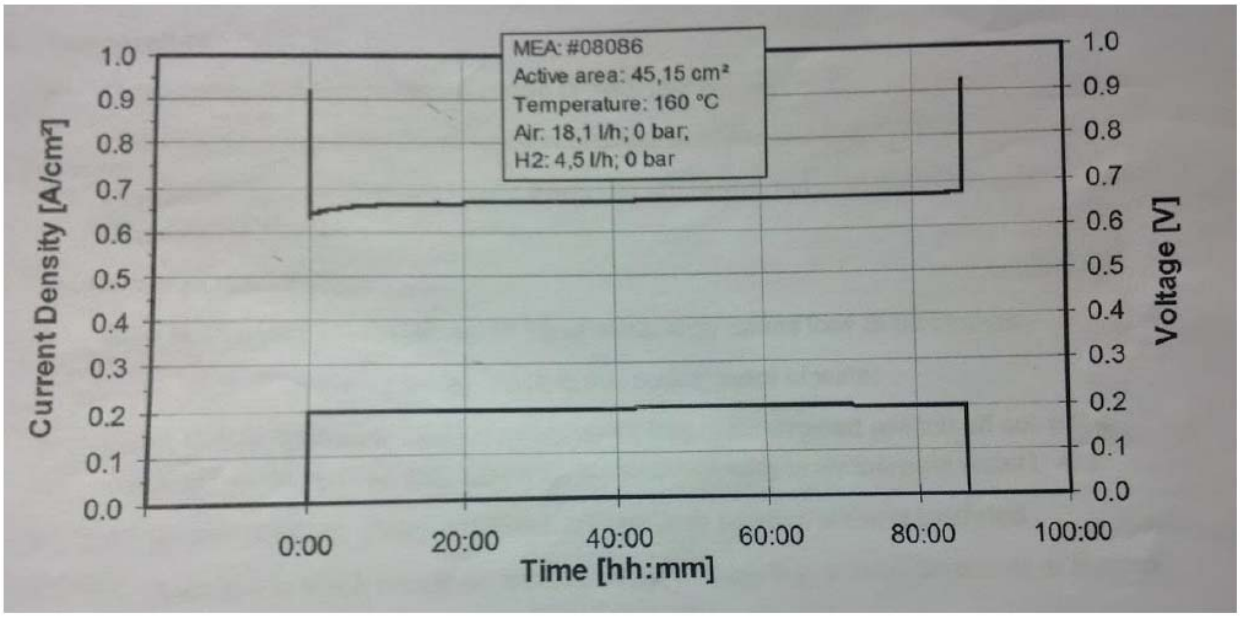

Figure 26. BASF hydrogen activation graph (Henschel, 2012).

As Figure 26, shows, in the first 50 hours, the performance of the MEA is improving. Based on the "Cell Assembling and Start-up Procedure for Celtec-P – MEA" from BASF Chemical Company. The activation steps are as follows:

1) Heat up fuel cell under dry hydrogen/oxygen at Open Circuit Voltage (OCV) to 160℃.
2) After reaching the temperature, go to 0.09 A/cm^2 current density. The pressure both of hydrogen flow and oxygen feed should keep at 2 psi.
3) After 50 hours, hydrogen feed is switched to methanol flow at 1.5 ml/min. At the same time, keep the oxygen flow pressure at 2 psi to make sure that the pressure is the same on both sides. Change the current to 1 A.

4) After 16 to 18 hours, the MEA is ready for testing.

The hydrogen activation is to make the catalyst fully activated. Methanol activation is to distribute methanol across the entire active area of the cell so that it is ready to begin amperage-variation testing with methanol feed (Callaghan and Lind, 2014). After a test, low down the temperature of the fuel cell is lowered and nitrogen is fed on both sides of the fuel cell, to keep it in an inert environment overnight before next test. Inert environment is to keep the MEA fully activated during the break. Before next test, we just need to run a smaller activation as follows:

1) Heat up fuel cell under dry hydrogen/oxygen at OCV to 160℃.
2) After reaching the temperature, go to 0.09 A/cm^2 current density. The pressure of both of hydrogen flow and oxygen flow should be kept at 2 psi.
3) After 3-4 hours, if the voltage is stable, hydrogen feed is switched to methanol flow at 1.5 ml/min. At the same time, keep the oxygen flow pressure at 2 psi to make sure that the pressure is the same on both sides. Change the current to 1 A.
4) After 3-4 hours, if the voltage keeps oscillating in a specific region, the MEA is ready to test.

3.3 Testing of PBI-based MEAs

This project tested the PBI-based MEAs in DMFC in two different parts. The first is the investigation of performance at different methanol concentrations and temperatures. The second part involves an investigation test of the fuel cell oscillatory behavior at different methanol concentrations and temperatures.

3.3.1 The performance of single PBI-based MEA

The performance test of single PBI-based MEA used as a DMFC was based on the MEA celtec-1100, obtained from BASF. The goal was to investigate performance with different methanol concentrations of 1 mol/L, 5mol/L and 10mol/L, and different temperatures of 160 ℃, 170℃ and 180 ℃. Methanol feed was vaporized in the furnace and pumped into fuel cell in the vapor phase to avoid leaching of phosphoric acid electrolyte. The feed line of methanol was heated by heating tape to ensure complete vaporization and no condensation. The temperature setup for the furnace is higher than that of the fuel cell and the lower temperature section, which is close to the fuel cell. The temperature for the furnace is 20 ℃ higher than that of other parts.

When the test was begun, the same concentration of methanol was used with increasing operating temperature. The test was conducted at temperatures 160 ℃, 170℃ and 180 ℃ for every given methanol concentration. After increasing temperature, fuel cell was operated for 30 minutes to 1 hour to ensure that the system is stable. Then another polarization test could done. The methanol flow rate of these tests was manufactured at 1.5 ml/min. Pressure of the oxygen feed line was kept at 2 psi.

3.3.2 The oscillatory Behavior of single PBI-based MEA

The oscillation test of single PBI-based MEA also used the MEA celtec-1100. The goal was to investigate the behavior at different methanol concentrations of 1 mol/L, 3 mol/L, 5 mol/L, 7.5 mol/L, and 10mol/L and at different temperatures of 160 ℃, 170℃ and 180 ℃. The operating conditions were the same as the performance tests of single PBI-based MEA. First, constant

current scan was conducted. A constant current value was set and the oscillations of the voltage at this current were recorded. The test was run for 10 minutes and then waited 10 minutes for next test. Second, constant voltage scan was conducted. A constant voltage value was set and the oscillations of the current at this voltage were recorded. The test was also run for 10 minutes, and then waited for another 10 minutes for next test.

Chapter 4: Results and Discussions

4.1 The performance of single PBI-based MEA

4.1.2 Temperature effects

Temperature is an important operating condition for a fuel cell. The experiments to determine the effect of temperatures were run at each feed methanol concentration at the temperatures of 160℃, 170℃ and 180℃. The performance for 1 mol/L methanol at temperatures ranges from 160 ℃ to 180 ℃ is shown in Figure 27, which was got by current scan. The current scan is to input current from to zero to maximum, and increase 0.01A every 10 seconds. Data were record every one second. I operate different current scan in different conditions. Some are one time scan, which we can see one curve. Others are reverse current scan, which can see two curves.

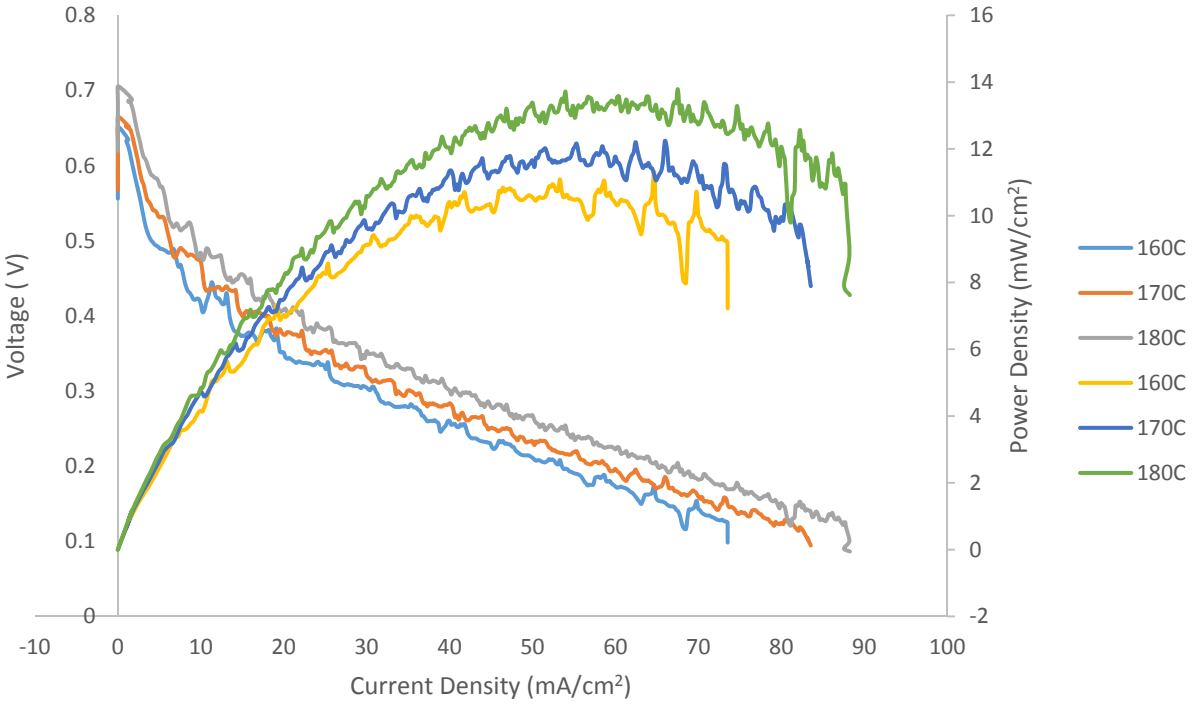

Figure 27. Polarization plot of 1 mol/L methanol as the anode feed, operated at temperatures from 160-180 ℃.

Figure 27, shows the cell voltage versus cell current density. Starting at a current density of 0, which corresponds to the open circuit voltage (OCV). As the current density increases, the voltage decreases. The power density obtained by multiplying voltage and current density versus current density is also shown at different temperatures and methanol concentrations. The power density starts at zero and reaches the maximum, and then begins to decrease as the current density increases. Further, we can also see that the temperature increases the performance of the MEA and OCV both increasing, as higher temperatures lead to higher electrode kinetics. Figure 27 also shows oscillatory behavior under all conditions with bigger oscillations at higher current density and higher temperature, which will be discussed in oscillations section. Figure 28 and Figure 29, show

similar polarization plots at 5 mol/L and 10 mol/L methanol. We can also see that as temperature increases the cell performance increases at the same time.

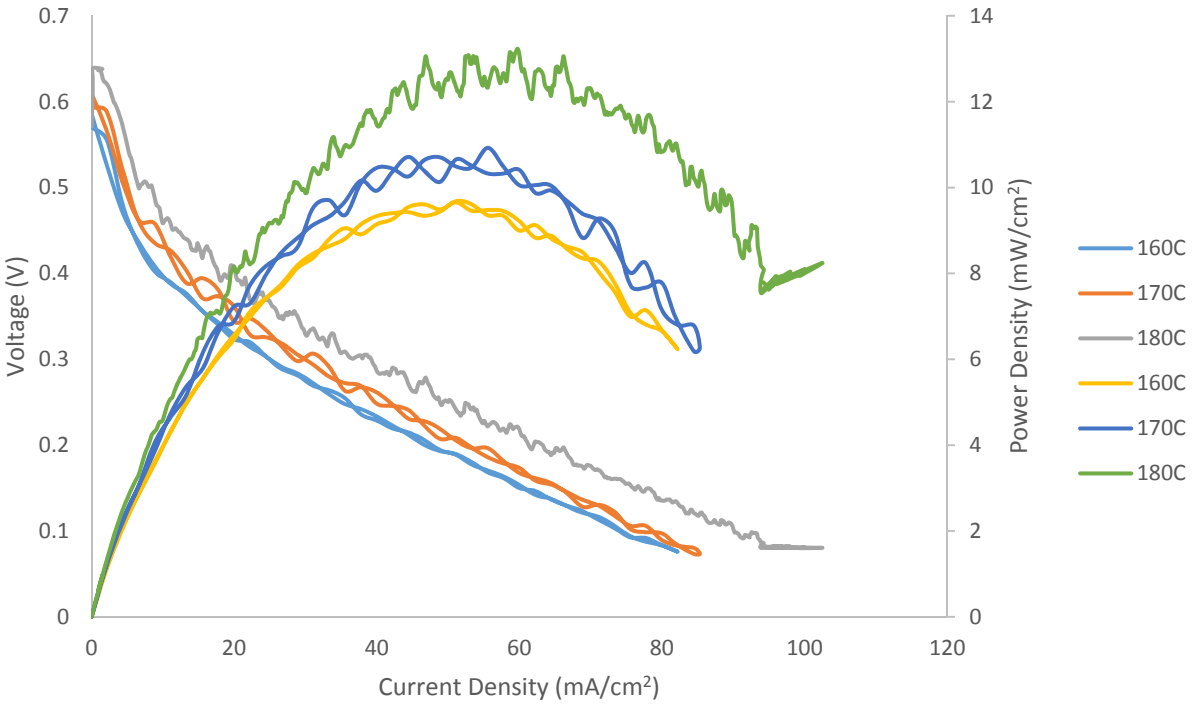

Figure 28. Polarization plot of 5 mol/L methanol as the anode feed, and run at temperatures from 160-180 ℃.

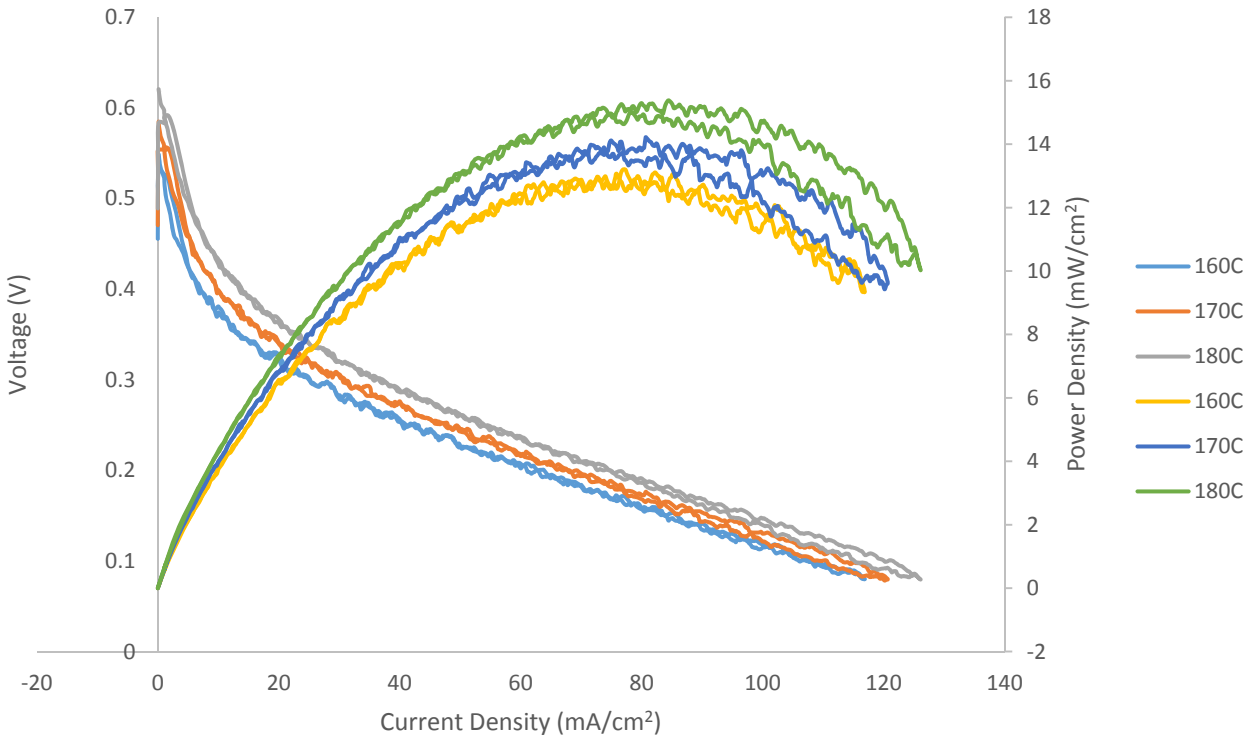

Figure 29. Polarization plot of 10 mol/L methanol as the anode feed, and run at temperatures from 160-180 ℃.

4.1.2 Methanol concentration effects

The two important factors that affect the performance of the direct methanol fuel cell are the operating temperature and the feed methanol concentration. In section 4.1.1, the effect of operating temperature was discussed. In this part, varying methanol concentrations at the same temperature were analyzed to study the effect of methanol concentration. Figure 30 is shown different concentrations of methanol vapor feed at 160 ℃.

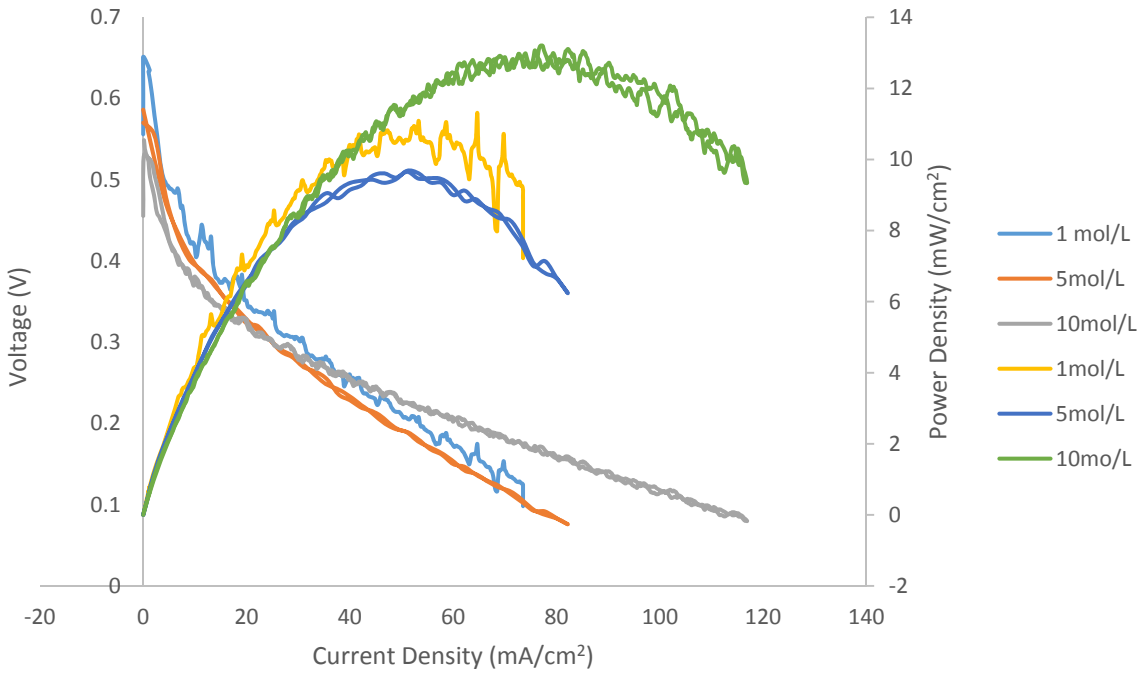

Figure 30. Polarization plot of 160 C methanol as the anode feed, and methanol concentration as 1 mol/L, 5 mol/L and 10 mol/L.

In Figure 30, it is seen that different concentrations of methanol, at low current density, the performance is almost the same. However, the larger concentration of methanol can reach higher current density and higher power density than the smaller methanol concentration feeds. Figure 30 also shows that the OCV decreases from the low methanol feed concentration to high methanol feed concentration, which may because the higher methanol concentration, the methanol crossover is higher. It is seen that the trends for different methanol concentrations are the same. Figure 31 and Figure 32 show the similar plots at temperature at 170 ℃ and 180 ℃.

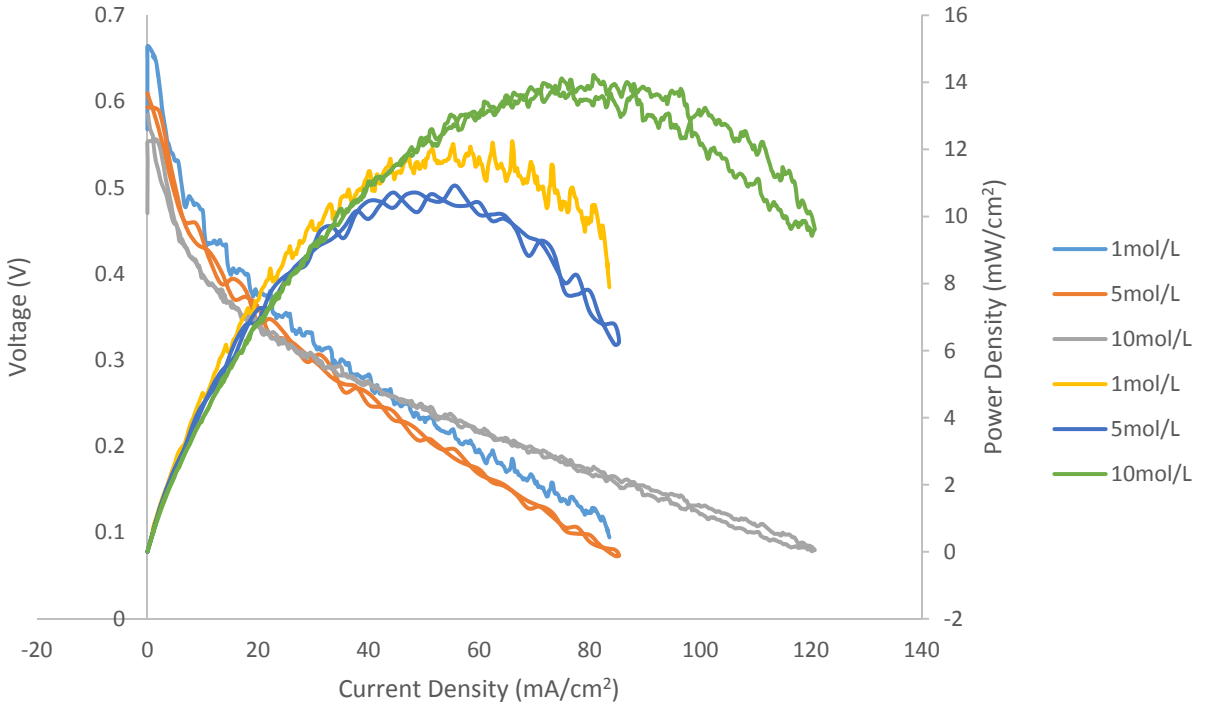

Figure 31. Polarization plot of 170 C methanol as the anode feed, and methanol concentration as 1 mol/L, 5 mol/L and 10 mol/L.

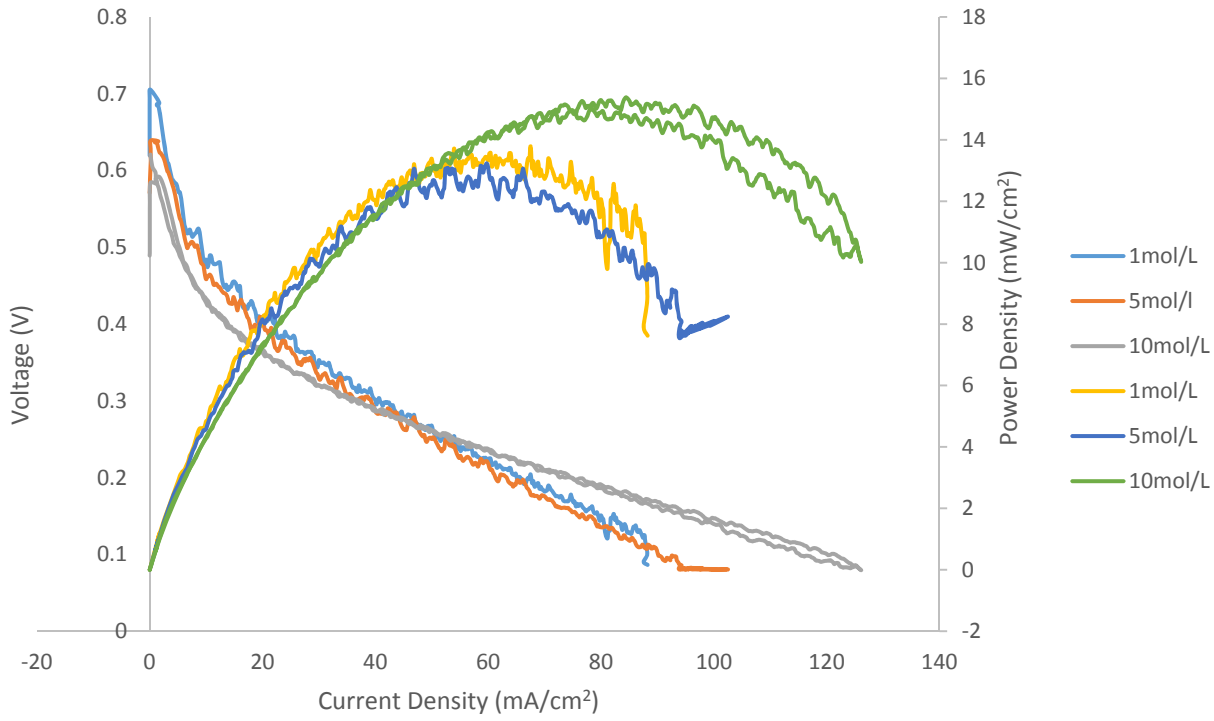

Figure 32. Polarization plot of 180 C methanol as the anode feed, and methanol concentration as 1 mol/L, 5 mol/L and 10 mol/L.

4.2 The oscillatory behavior of single PBI-based MEA

As mentioned above, when the performance of single PBI-based MEA was tested as a function of methanol concentration and temperature, voltage oscillations were found. Thus, in this section, constant current and constant voltage scans were run to further study this oscillation phenomena.

4.2.1 Constant current scan

There may be three factors, which affect the oscillations in a constant current scan mode, namely, current density, methanol concentration, and temperature. Thus, in this section, several groups of experiments were conducted to investigate these. Figure 33 shows the oscillations for a 3 mol/L methanol feed constant current densities for 30 minutes at 160 ℃.

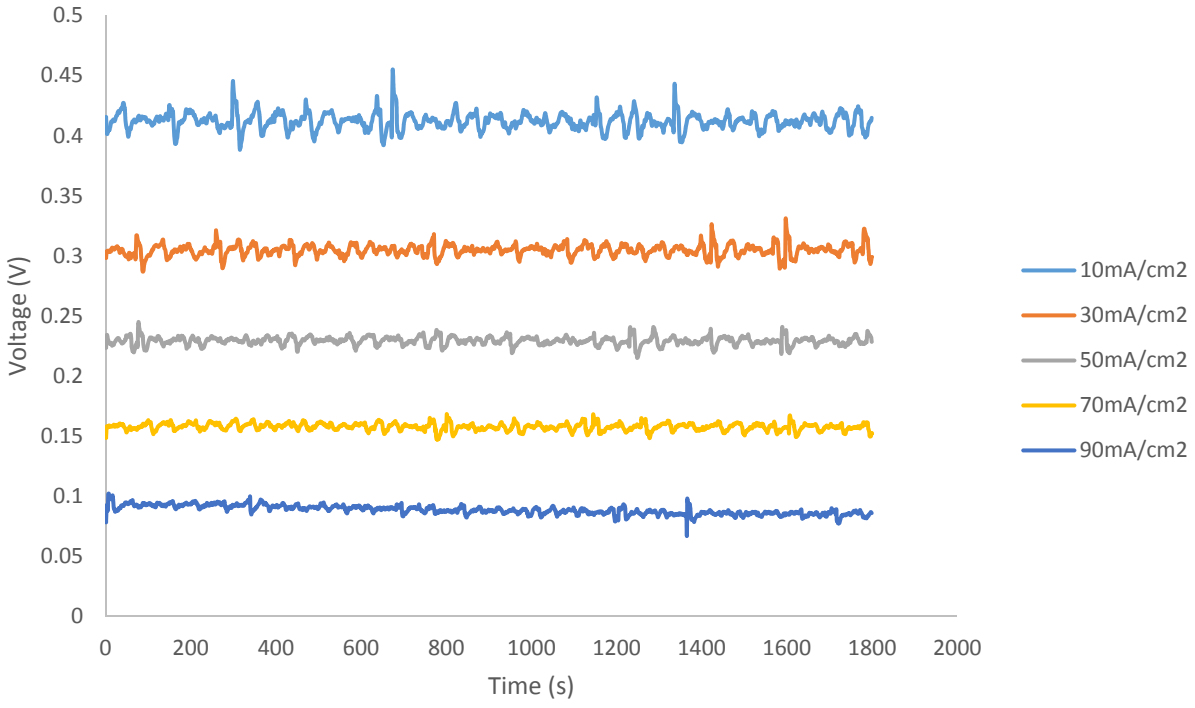

Figure 33. Oscillatory behavior of voltage at constant current densities at 160℃ and 3mol/L methanol.

In Figure 33, oscillatory temperature and methanol concentration and change the current density. It is seen that the voltage oscillation amplitude became smaller when the current density was increased. For the 30 minutes test, the oscillation pattern is the same, so that the test time for subsequent tests was shortened to 10 minutes. Figure 34 and Figure 35 show for different temperatures, the oscillations of 3 mol/L methanol feed at different current densities.

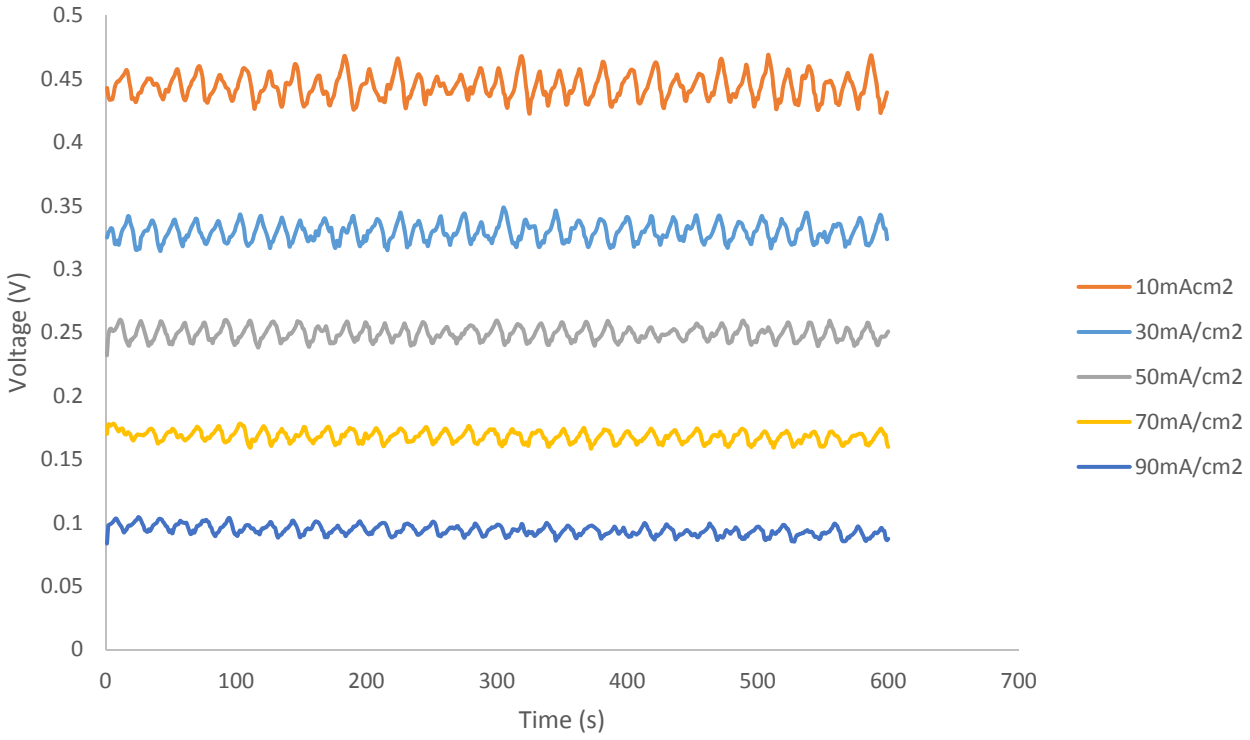

Figure 34. Oscillatory behavior of voltage at constant current densities at 170℃ and 3mol/L methanol.

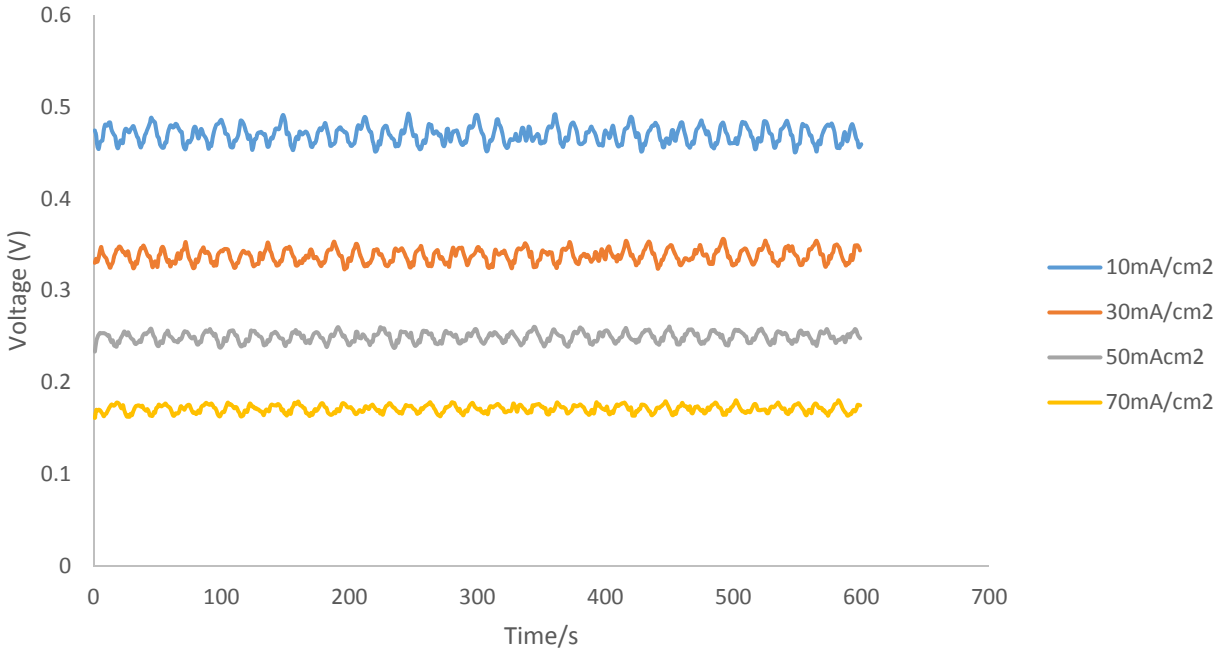

Figure 35. Oscillatory behavior of voltage at constant current densities at 180℃ and 3mol/L methanol.

We can investigate the effect of temperature on the voltage oscillations by comparing Figures 33, Figure 34 and Figure 35. From these figures, it is clear that the temperature has only a small influence on the voltage oscillation period as amplitude in the range of temperature investigated.

Then similar experiments were run to test the oscillations at 5 mol/L, 7.5 mol/L and 10 mol/L methanol concentration at temperatures of 160℃, 170℃ and 180℃ at different constant current densities, which are shown in the following figures.

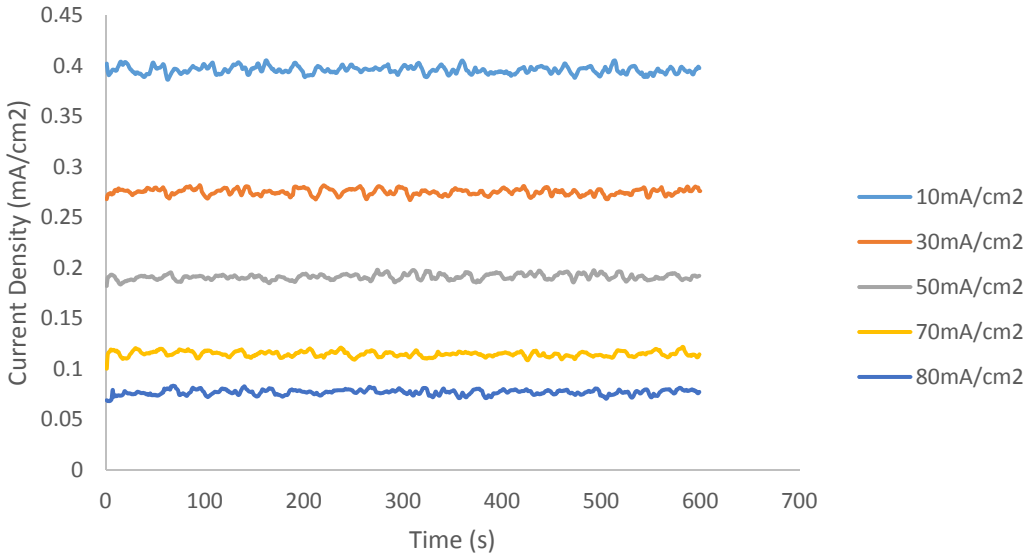

Figure 36. Oscillatory behavior of voltage at constant current densities at 160 ℃ and 5mol/L methanol.

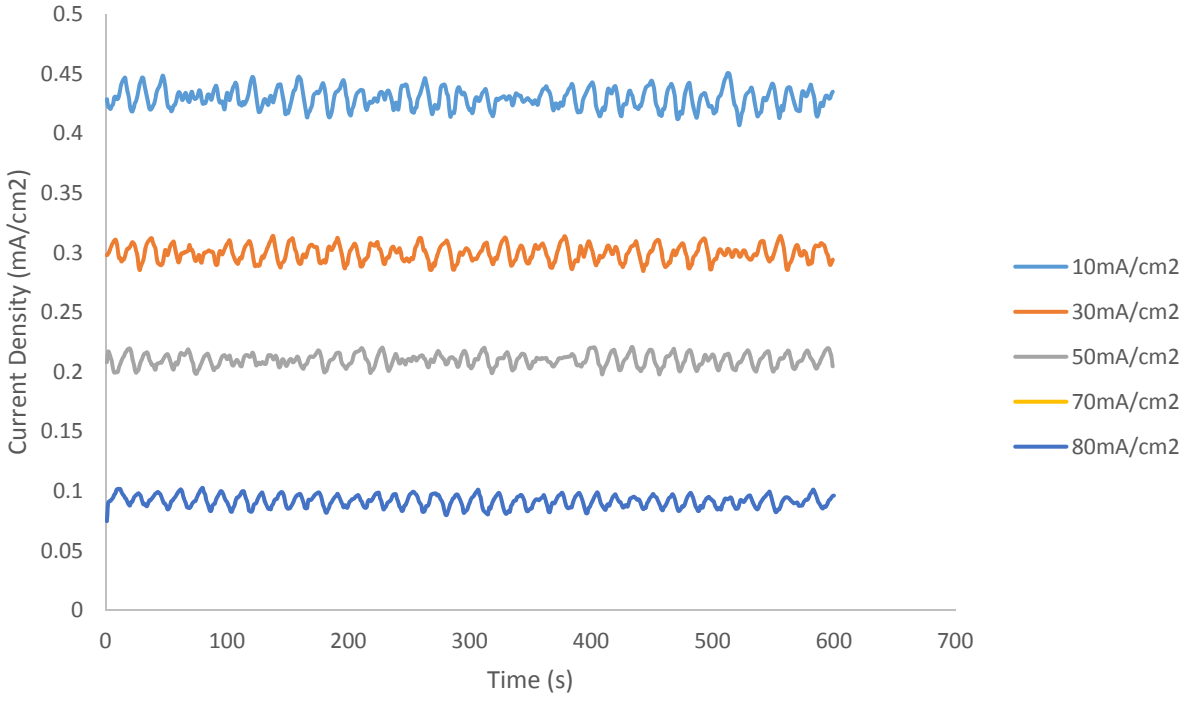

Figure 37. Oscillatory behavior of voltage at constant current densities at 170 ℃ and 5mol/L methanol.

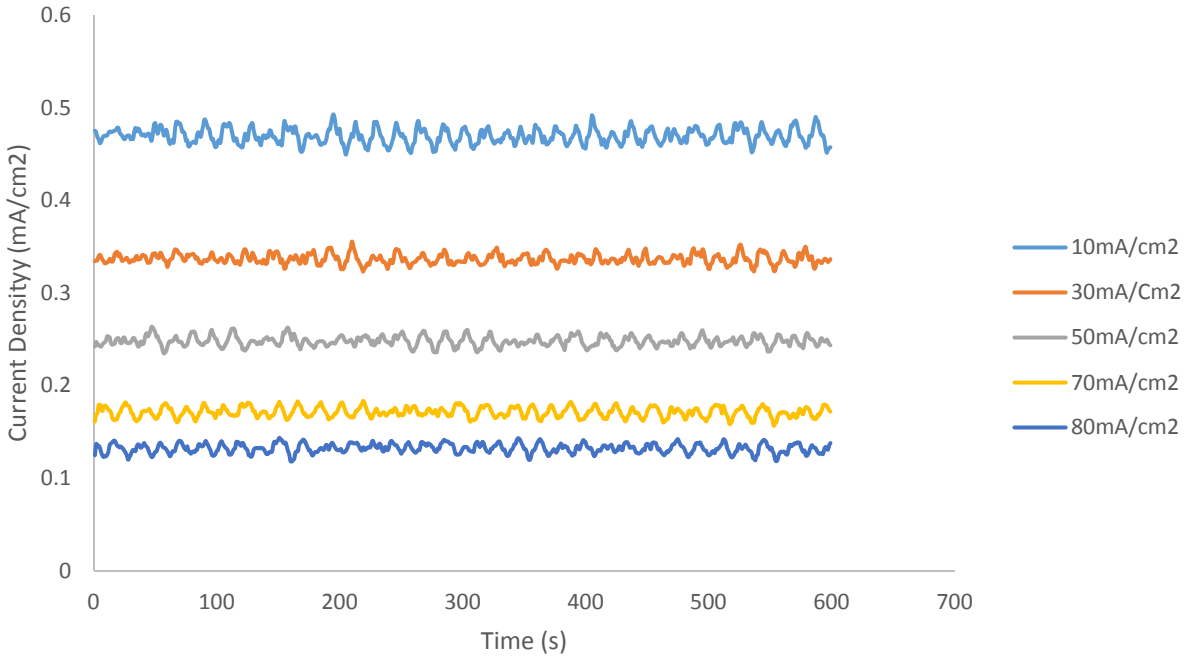

Figure 38. Oscillatory behavior of voltage at constant current densities at 180℃ and 5mol/L methanol.

.

.

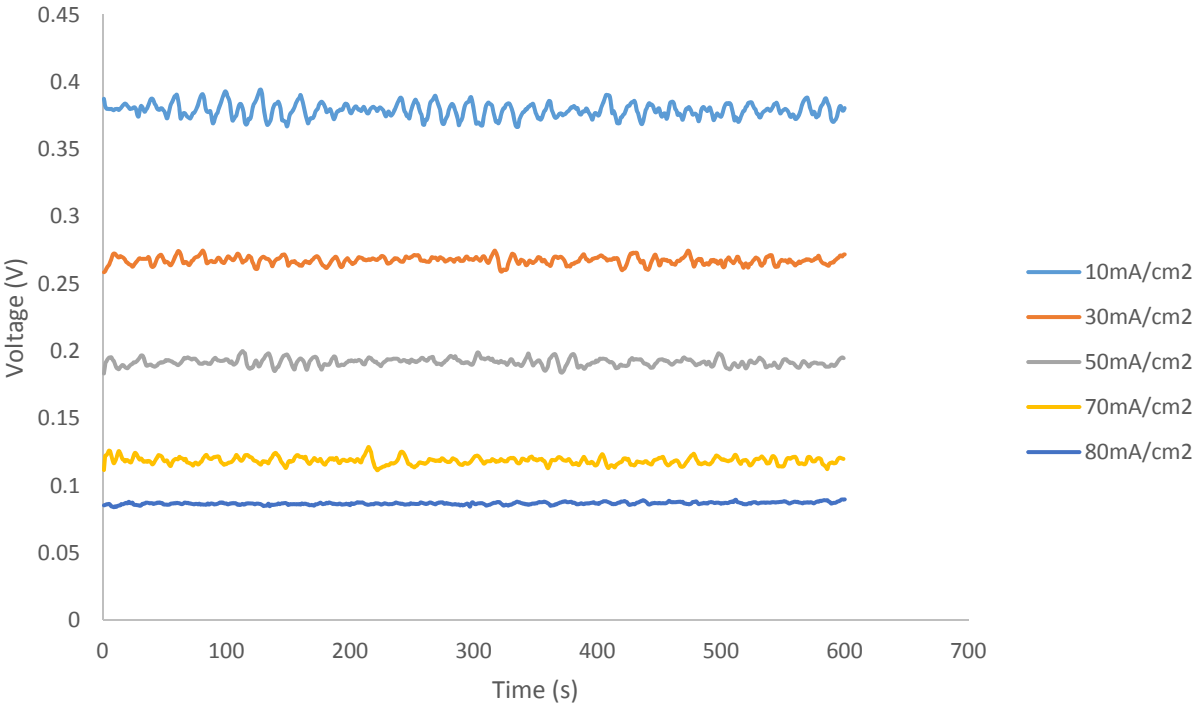

Figure 39. Oscillatory behavior of voltage at constant current densities at 160℃ and 7.5mol/L methanol.

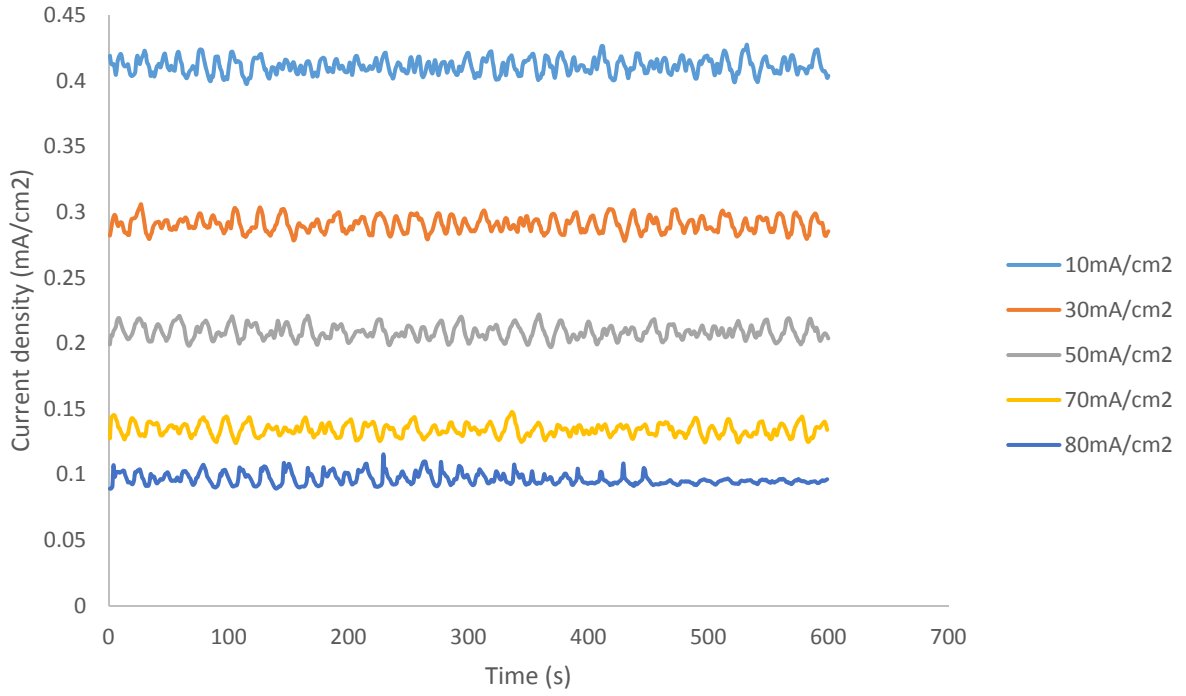

Figure 40. Oscillatory behavior of voltage at constant current densities at 170℃ and 7.5mol/L methanol.

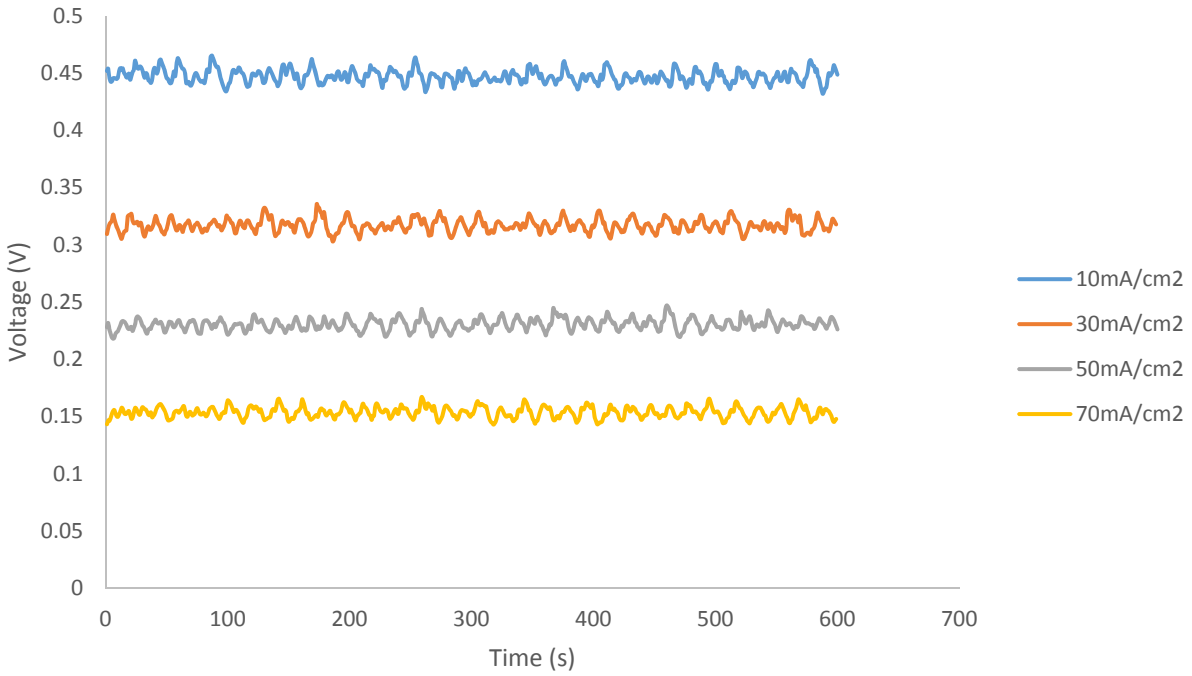

Figure 41. Oscillatory behavior of voltage at constant current densities at 180℃ and 7.5mol/L methanol

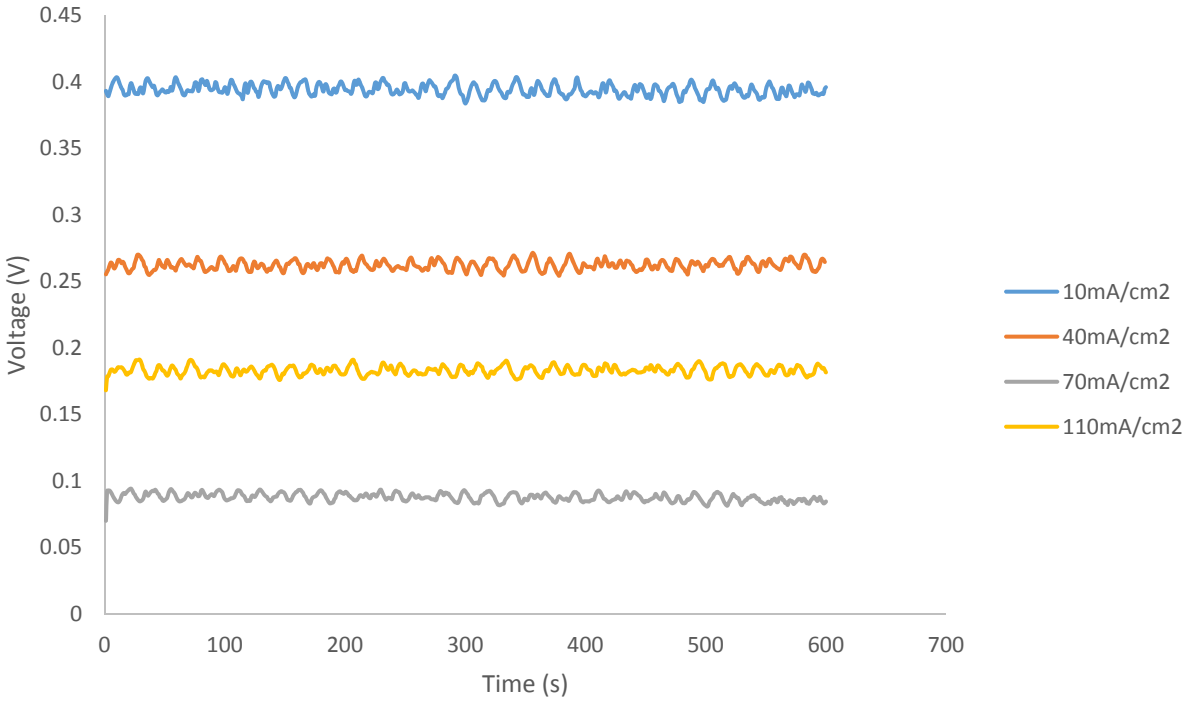

Figure 42. Oscillatory behavior of voltage at constant current densities at 160℃ and 10mol/L methanol

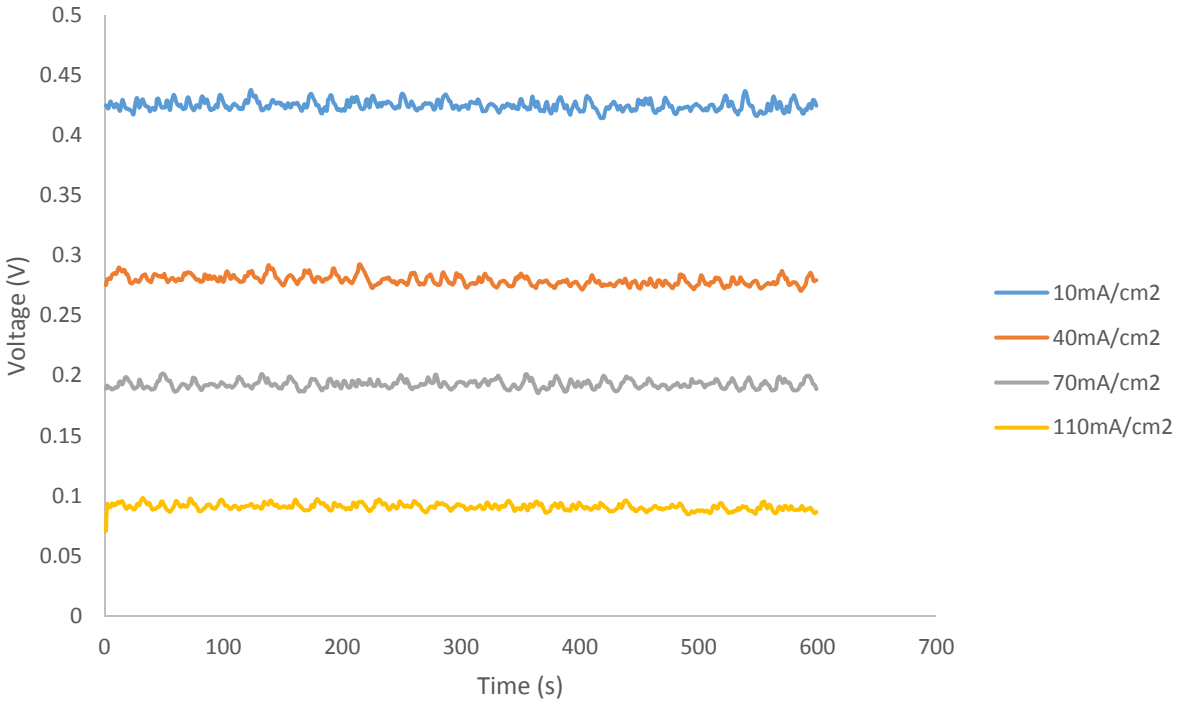

Figure 43. Oscillatory behavior of voltage at constant current densities at 170℃ and 10mol/L methanol.

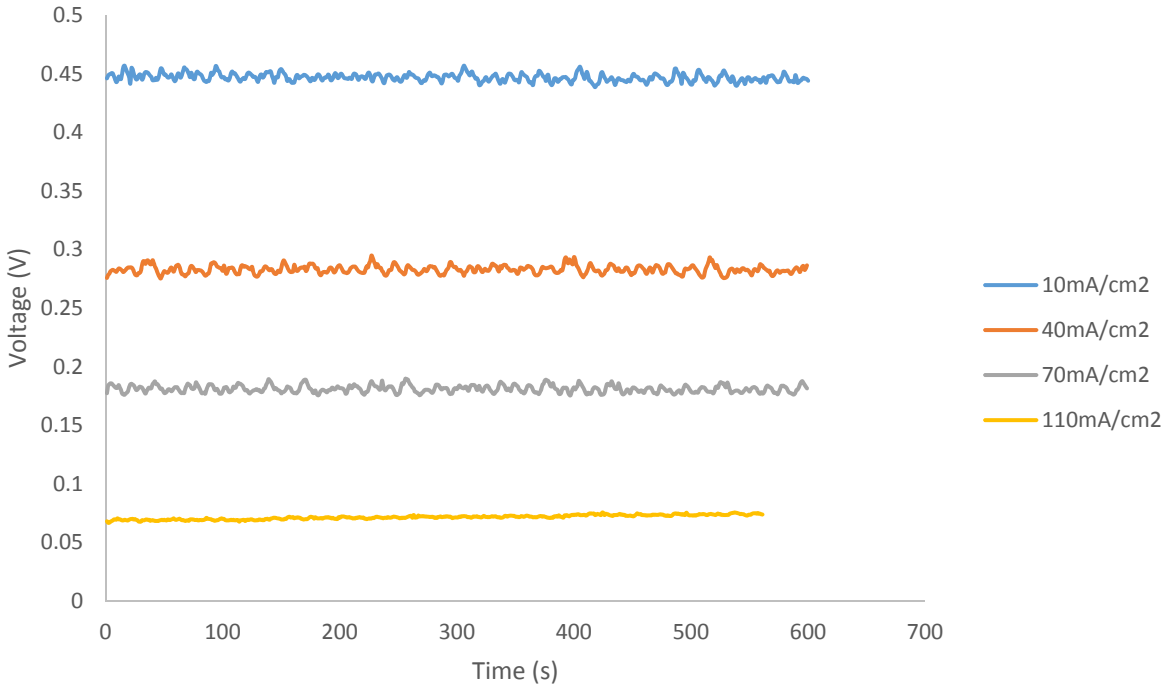

Figure 44. Oscillatory behavior of voltage at constant current densities at 180℃ and 10mol/L methanol.

Figure 34, 37, 40 and 33 show oscillations for different concentrations of methanol at same temperature and current density. From these figures, it appears that methanol concentration does not significantly affect the voltage oscillation.

4.2.2 Constant voltage scan

To see if the oscillatory behavior was affected. Experiments were conducted at constant voltage. There may be also three factors which affect the oscillation in constant voltage scan, namely, voltage, methanol concentration and temperature, so that different groups of experiments were conducted to compare the effects of voltage, methanol concentration and temperature. Figure 45 shows the current density oscillation for 3 mol/L methanol feed at constant voltage scan at different cell voltages for 30 minutes at 160 ℃

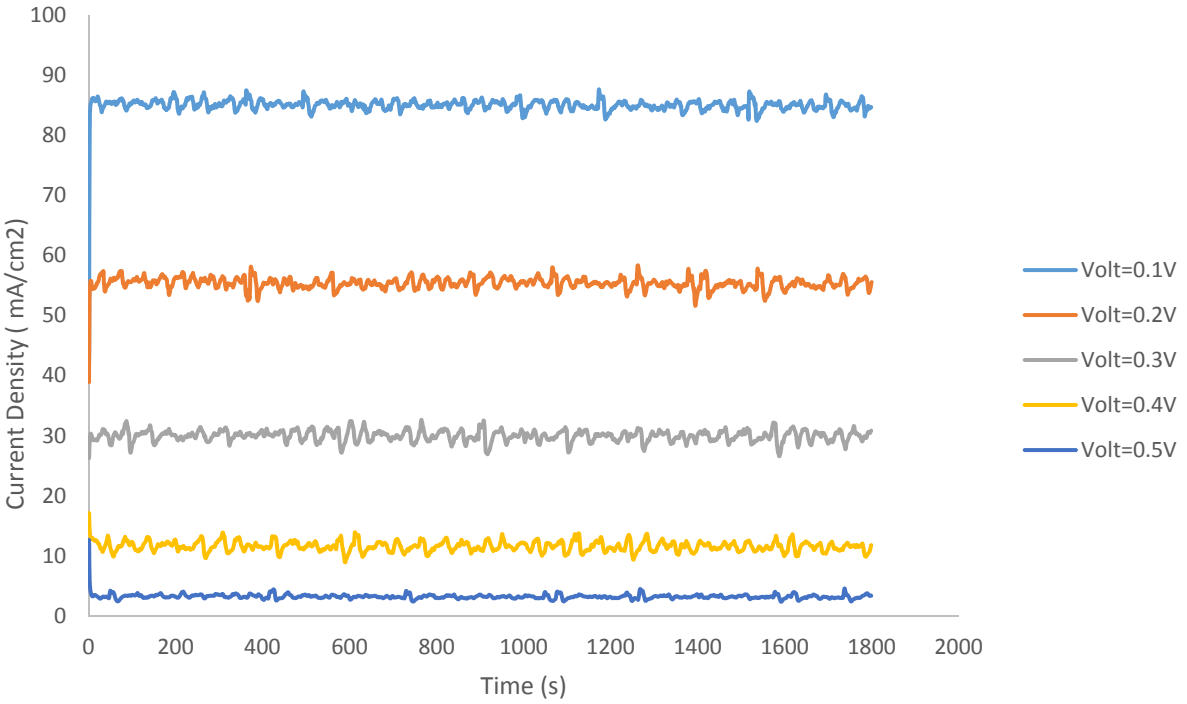

Figure 45. Oscillatory behavior of current density at constant voltages at 160℃ and 3mol/L methanol.

From Figure 45, it is evident that the oscillations behavior of current density did not change significantly, when the cell voltage is changed. For the 30 minutes test, the oscillation pattern is unchanged, so that the test time was shortened to 10 minutes for the remaining tests. Figure 46 and Figure 47 show at different temperatures the oscillations for 3 mol/L methanol feed at different cell voltages, which show that the pattern as Figure 45.

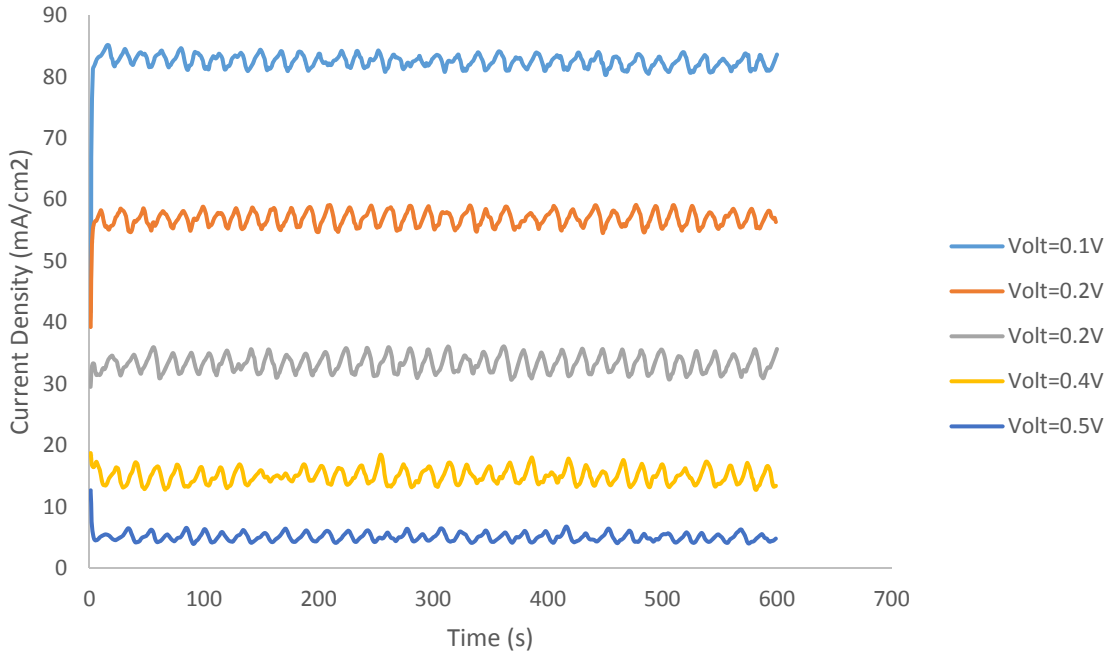

Figure 46. Oscillatory behavior of current density at constant voltages at 170℃ and 3mol/L methanol.

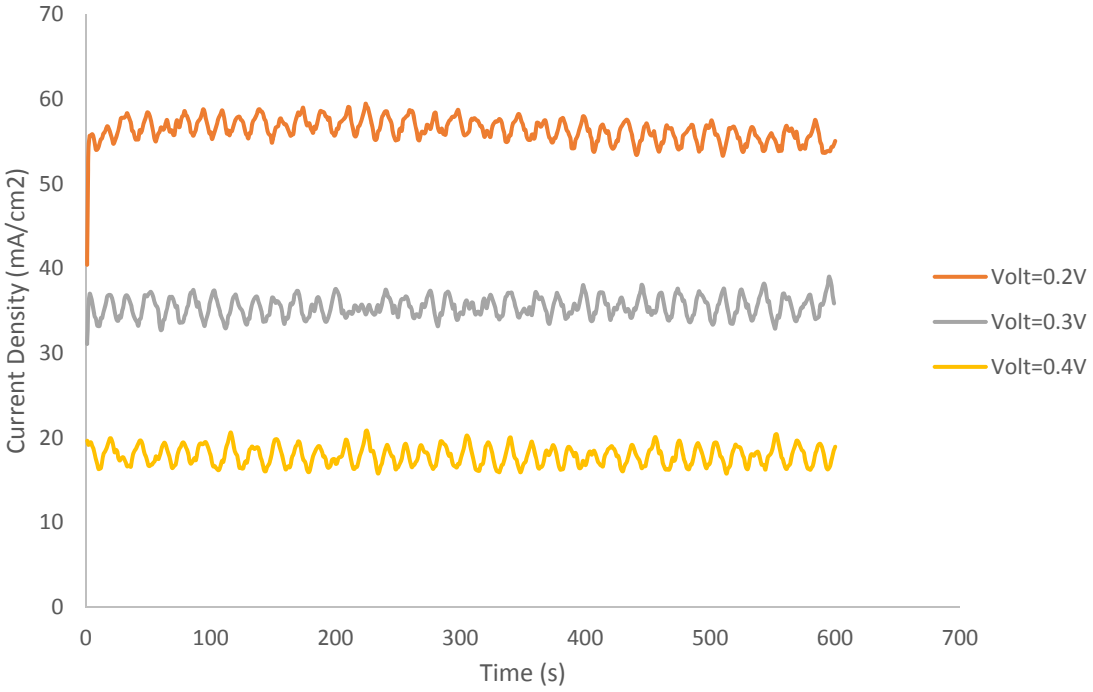

Figure 47. Oscillatory behavior of current density at constant voltages at 180℃ and 3mol/L methanol.

We can find the effect of temperature on the current density oscillations at constant voltages by comparing Figures 45, 46 and 47. From these figures, it is seen that the temperature makes only a small influence on the current density oscillation pattern, when cell is operated at a constant voltage.

Similar experiments were conducted to test the current density oscillations for 5 mol/L, 7.5 mol/L and 10 mol/L methanol at temperatures of 160℃, 170℃ and 180℃ at different cell voltages, which are shown in the following figures.

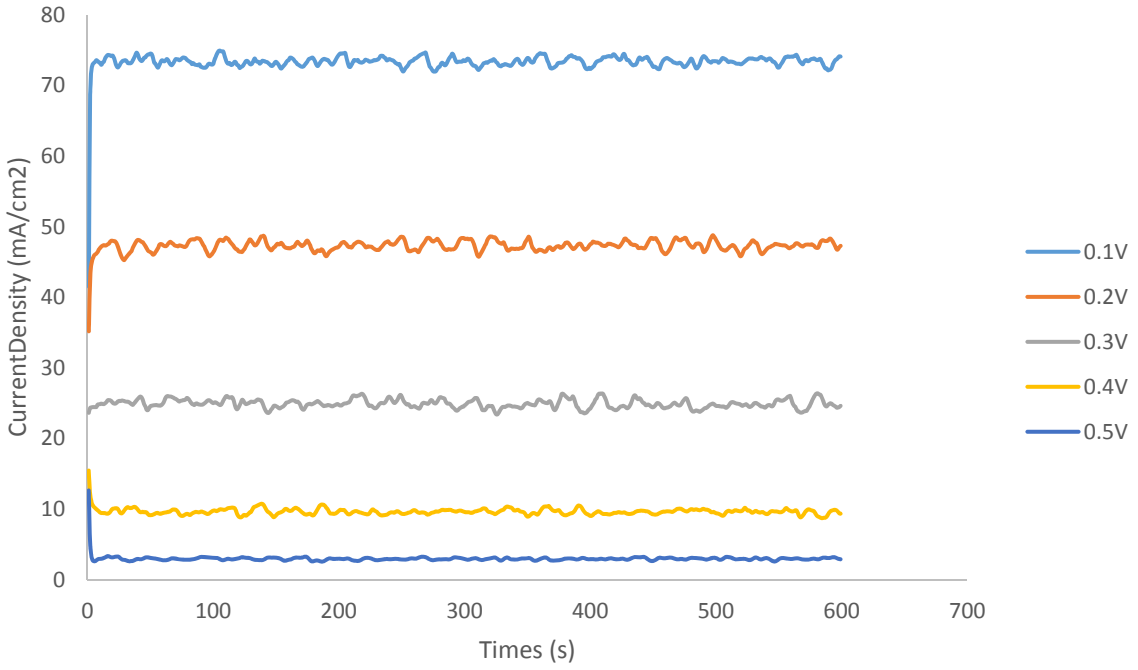

Figure 48. Oscillatory behavior of current density at constant voltages at 160℃ and 5mol/L methanol.

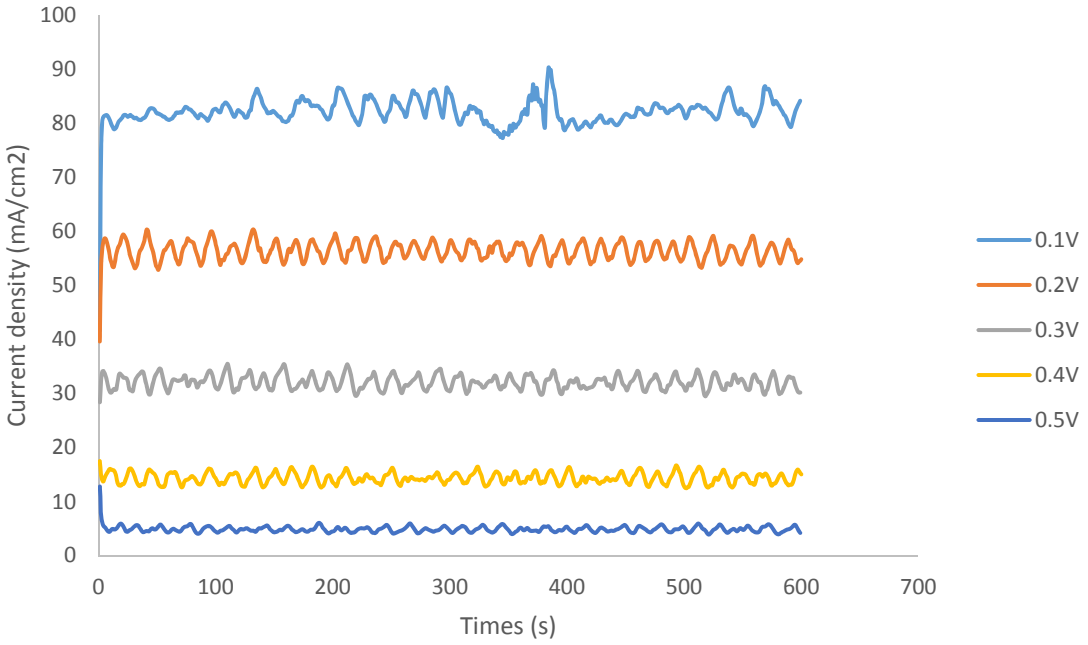

Figure 49. Oscillatory behavior of current density at constant voltages at 170℃ and 5mol/L methanol.

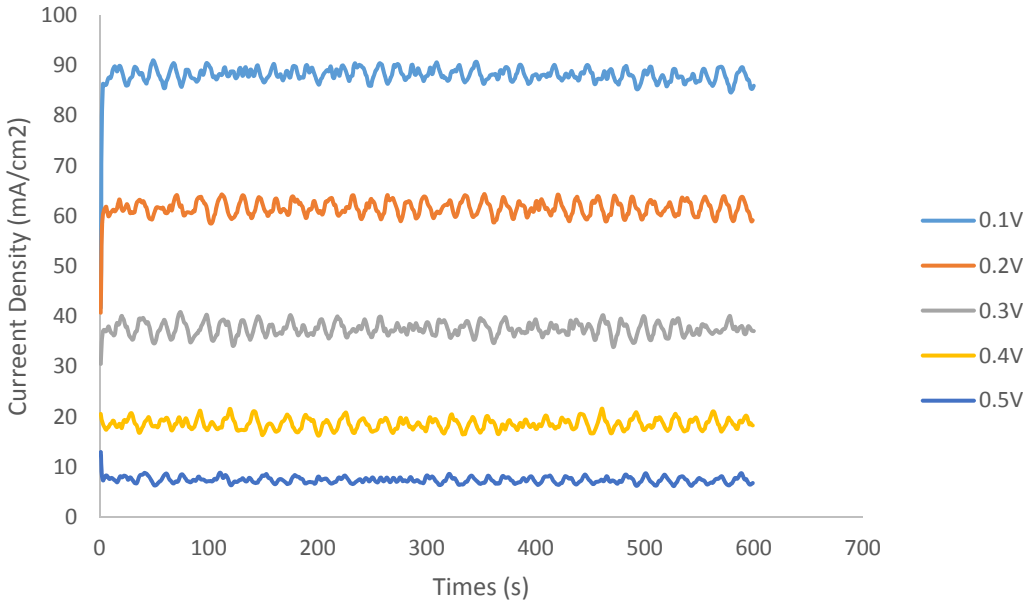

Figure 50. Oscillatory behavior of current density at constant voltages at 180℃ and 5mol/L methanol.

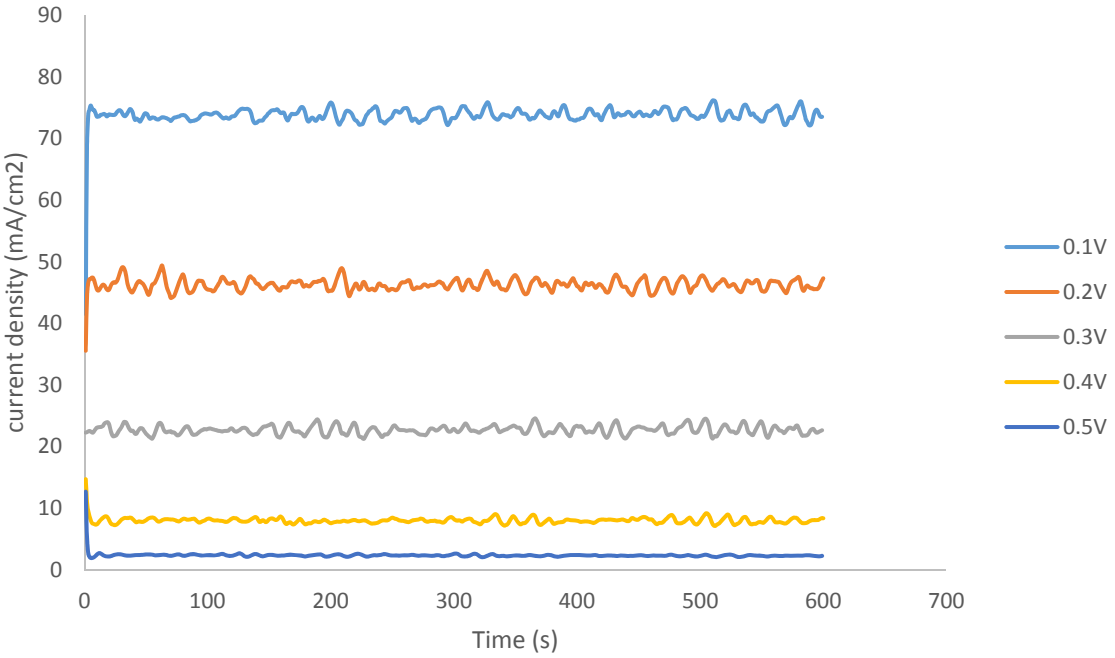

Figure 51. Oscillatory behavior of current density at constant voltages at 160 ℃ and 7.5mol/L methanol.

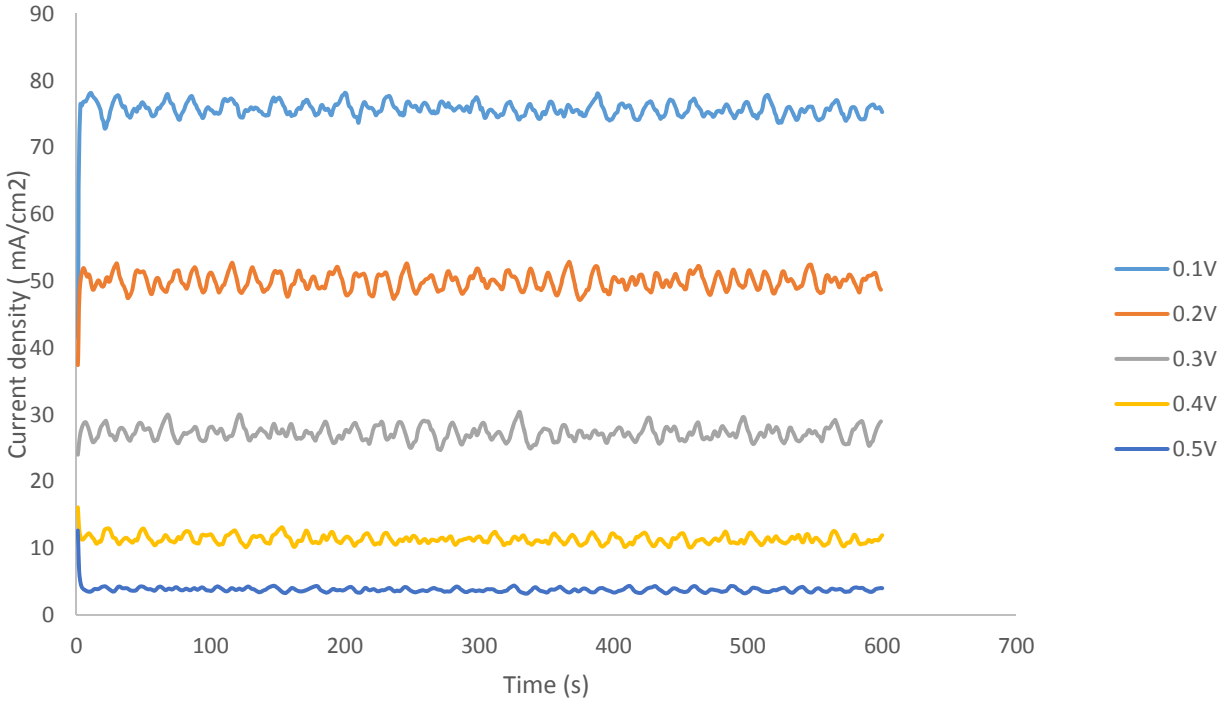

Figure 52. Oscillatory behavior of current density at constant voltages at 170 ℃ and 7.5mol/L methanol.

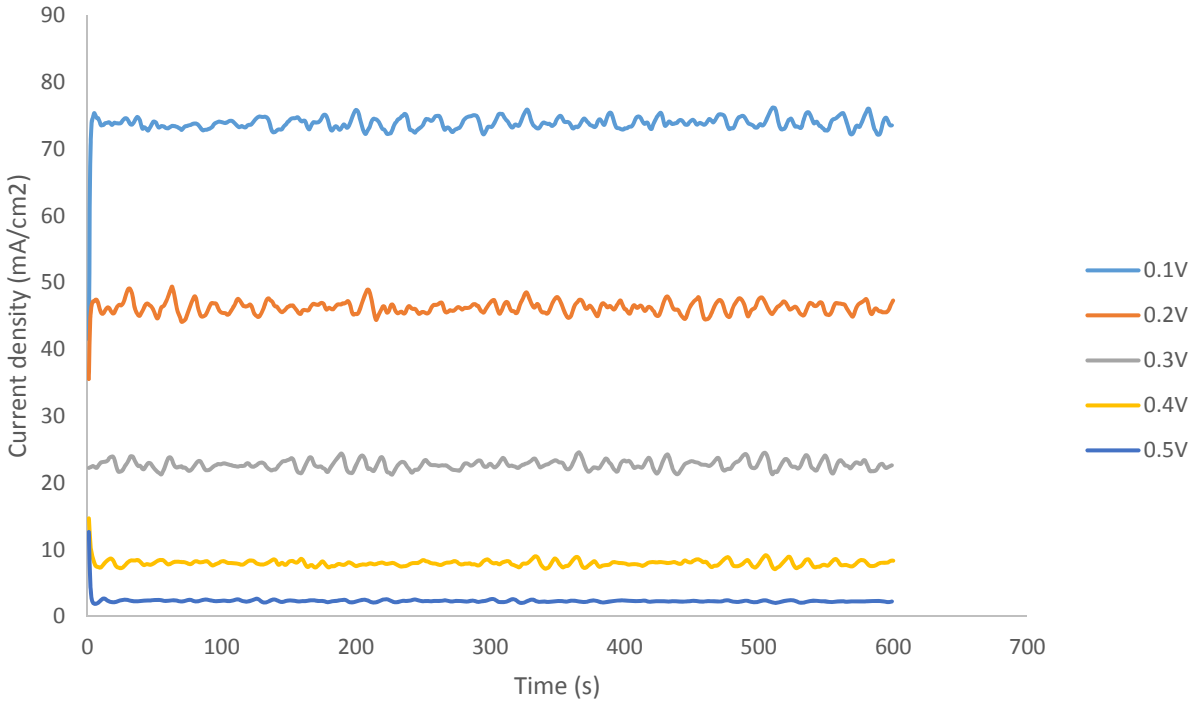

Figure 53. Oscillatory behavior of current density at constant voltages at 180 ℃ and 7.5mol/L methanol.

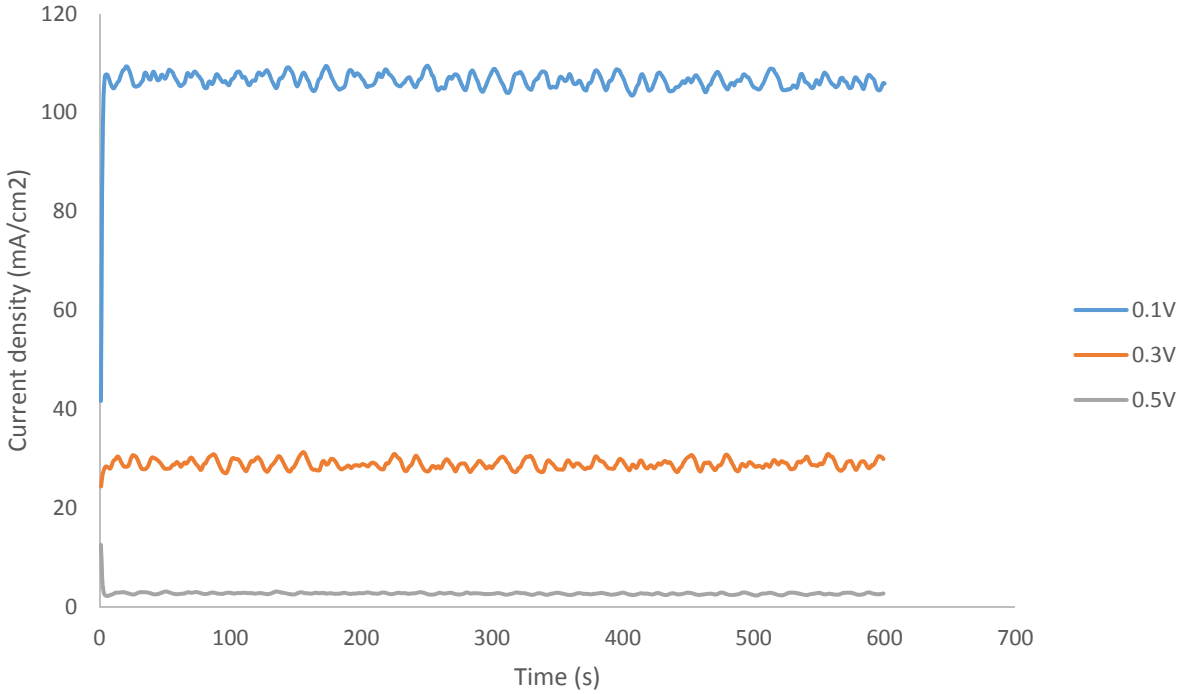

Figure 54. Oscillatory behavior of current density at constant voltages at 160 ℃ and 10 mol/L methanol.

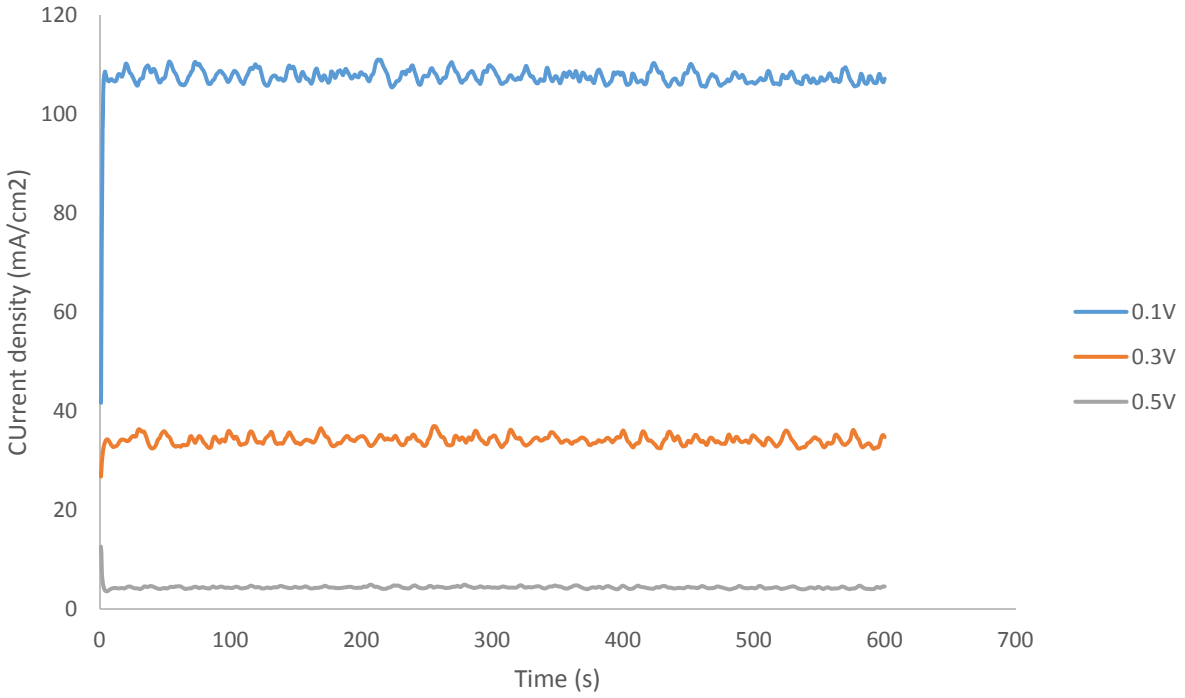

Figure 55. Oscillatory behavior of current density at constant voltages at 170℃ and 10mol/L methanol.

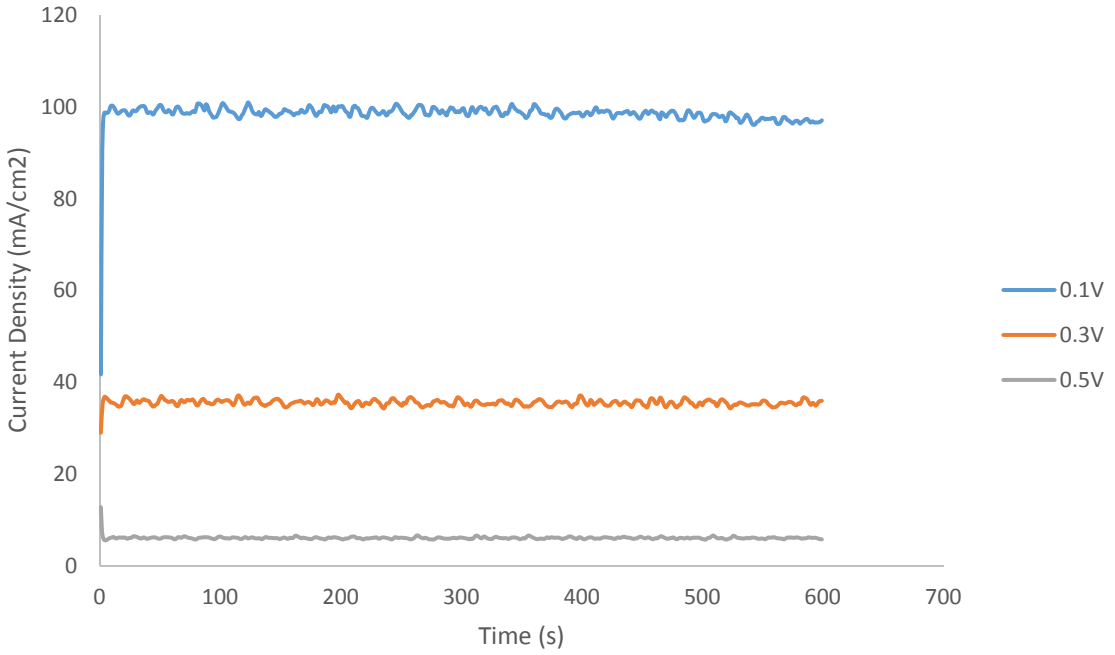

Figure 56. Oscillatory behavior of current density at constant voltages at 180℃ and 10mol/L methanol.

Figure 46, 49, 52 and 5 show oscillatory behavior at different concentrations of methanol at same temperature and constant cell voltages. From these figures, it is seen that methanol concentration is not a significant factor for current density oscillations, when run at constant cell voltage. The oscillatory behaviors show the cycle of CO adsorbing and cleaning. CO is one of the intermediate products in methanol oxidation. CO can strongly adsorb on the surface of Pt catalysts and block the active sites, which will lead to the decline of cell potential or current density. Thus, it is seen the voltage and current density decrease in these figures. At the temperature range of 160-180°C, CO can desorb partly from the catalysts, and the voltage or current density increases. Thus, it is seen as the oscillatory behavior for the CO adsorb and clean cycle.

Chapter 5: Conclusions and Recommendations

Fuel cells are one of the most efficient methods to generate electric power now, which is also an environment-friendly way to reduce the air pollution. Fuel cells can be used in many fields, such as large-scale power generation, on-site emergency power supply, fuel cell vehicles and personal computer or cell phone. Methanol as a liquid fuel has a number of advantages as compared with hydrogen fuel. Methanol is a liquid, which is easy to store and transport, and also has a high energy density. The conventional DMFCs are based on Nafion membrane. However, methanol crossover and catalyst poisoning are two big issues for requiring high catalyst loading and operation with dilute methanol. PBI-based membrane can work at higher temperature with vapor phase methanol feed, and can provide higher kinetics and lower methanol crossover. Thus, PBI-based MEA, Celtec-P 1100 was tested in this project to investigate DMFC performance.

This thesis investigated two goals for PBI-Phosphoric acid based MEA for DMFC. First is the effect of temperature and methanol concentration. In the temperature range of 160-180 ℃, as the temperature increased, the performance of the PBI-Phosphoric acid based DMFCs increased, because higher temperatures lead to higher kinetics and lower overpotentials. Further, at high temperature the effect of methanol feed concentration is small. The reason may be that higher concentration means more fuels, but it also increases methanol crossover. Well known, methanol concentration gradient is an important factor for methanol crossover. The second goal was a study of the oscillation phenomenon in constant current and constant voltage. CO is one of the intermediate products, which can poison the catalysts. It is theorized that these oscillations

show catalysts poisoning and cleaning cycles, which is replaced apparently for the first time for DMFCs.

References

Ahmed, M. and Dincer, I., 2011. A review on methanol crossover in direct methanol fuel cells: challenges and achievements. *International Journal of Energy research*, 35, 1213-1228(2011)

Arico, A., S., Baglio, V. and Antonucci, V., 2009. Direct Methanol Fuel Cells: History, Status and Perspectives in Electrocatalysis of Direct Methanol Fuel Cells: From Fundamentals to Applications (eds H. Liu and J. Zhang). Wiley-VCH Verlag GmbH & Co.KGaA, Weiheim, Germany.

Arisetty, S., Krewer, U., Advani, S., G. and Prasad, A., K., 2010. Coupling of kinetic and mass transfer processes in direct methanol fuel cells. *Journal of the Electrochemical Society*, 157, B1143-B1455 (2010)

Bagotsky, V.S., 2012. Fuel Cells Problems and Solutions, Second Edition. Hoboken, New Jersey: John Wiley & Sons, Inc.

Baldauf, M. and Preidel, W., 1999. Status of the development of a direct methanol fuel cell. *Journal of Power Sources* 84, 161-166(1999)

Barbir, F., 1997, Fuel Cell Tutorial, presented at Future Car Challenge Workshop, Dearborn, MI, October 25-26, 1997.

Barbir, F., 2005. PEM Fuel Cells: Theory and Practice. Elsevier Academic Press, New York, 2005.

BASF Chemical Company, 2012. Cell assembling and start-up procedure for Celtec-P MEA.

Callaghan, S. and Lind, W., 2014. Analysis of Polybenzimidazole feasibility in a Direct Methanol Fuel Cell utilizing temperature and methanol concentrations. Worcester Polytechnic Institue.

Carrette, L., Friedrich, K., Stimming, U., 2000. Fuel Cells: Principles, Types, Fuels and Applications. *Chemphyschem* 1, 162-193(2000)

Chen, C., Y. and Yang, P., 2003. Performance of an air-breathing direct methanol fuel cell. *Journal of Power Source*, 123, 37-42(2003).

Datta, R. 2014. Fuel cell Technology Course Note.

Debe, M.K., 2012. Electrocatalyst approaches and challenges for automotive fuel cells. *Nature* 486, 43-51(2012)

DuPont Fuel Cells, http://www2.dupont.com/FuelCells/en_US/index.html

Franklin, G., W. and Connolly, D.J, 1966. Fluorocarbon Vinyl Ether Polymers. U.S. Patent 3282875 A

Gierke, T., D. et al, 1982. Perfluorinated Ionomer Membranes, ACS Symposium Series, 283 (1982)

Gottesfeld, S. and Zawodzinski, T., A., 1997. Polymer Electrolyte Fuel Cells. Wiley-VCH, New York, 1997.

Hamnett, A., 1997. Mechanism and electrocatalysis in the direct methanol fuel cell. *Catalysis Today* 38, 445-457(1997)

Heinzel, A. and Barrgan, V., M., 1999. A review of the state-of-the-art of the methanol crossover in direct methanol fuel cells. *Journal of Power Sources,* 84, 70-74(1999).

Henschel, C., 2012. Cell assembling and start-up procedure for Celtec-P-MEA. BASF Chemical Company.

Hoogers, G., 2003. Fuel Cell Technology Hand Book. Danvers, MA: CRC Press LLC.

Kreuer, K., Rabenau, A. and Weppner, W., 1982. Vehicle Mechanism, A New Model for the Interpretation of the Conductivity of Fast Proton Conductors. Angewandte Chemie, 21, 208(1982)

Larminie, J. and Dicks, A., 2003. Fuel cell systems explained, second edition. Chichester, England, John Wiley & Sons, ltd.

Leonard, N., J., 1994. Carl Shipp Marvel Biographical Memoir. National Academy of Sciences.

Li, W., Zhou, W., Li, H., Zhou, Z., Zhou, B., Sun, G. and Xin, Q., 2004. Nano-stuctured Pt-Fe/C as cathode catalyst in direct methanol fuel cell. *Electrochimica Acta,* 49, 1045-1055(2004)

Lobato, J., Canizares, P., Rodrigo, M., A., Linares, J., J. and Lopez-Vizcaino, R., 2008. Performance of a vapor-fed Polybenzimidazole (PBI)-based direct methanol fuel cell. *Energy & Fuels,* 22, 3335-3345(2008).

McNicol, B., D., Rand, D., A., J. and Williams, K., R., 1999. Direct methanol-air fuel cells for road transportation. *Journal of Power Sources* 83, 15-31(1999)

Mukerjee, S., Srinivasan, S., Soriaga, M., P. and McBreen, J., 1995. Role of structural and electronic properties of Pt alloys on electrocatalysis of oxygen reduction. *Journal of Electrochemical Society*, 142, 1409-1422(1995)

O'Hayre, R., Cha, S., Colella, W., G. and F., B., 2006. Fuel Cell Fundamentals. Hoboken, New Jersey: John Wiley & Sons, Inc.

Olah, G., A., 2005. Beyond Oil and Gas: The Methanol Economy. *Angewandte Chemie Interantional Edition*, 44, 2636-2639(2005).

Pivovar, B., S., Bender, G., Davey, J., R. and Zelenay, P., 2003. Methanol crossover in direct methanol fuel cell systems. Los Alamos National Laboratory.

Reeve, R., W., Christensen, P., A., Hamnett, A., Haydock, A. and Roy, S., C., 1998. Methanol tolerant oxygen reduction catalysts based on transition metal sulfides. *Journal of Electrochemical Society,* 145, 3643-3471(1998)

Reeve, R.W., Christensen, P., A., Dickinson, A., J., Hamnett, A. and Scott, K., 2000. Methanol-tolerant oxygen reduction catalysts based on transition metal sulfides and their application to the study of methanol permeation. *Electrochimica Acta,* 45, 4237-4250(2000)

Rodrigues, A. et al, 1997. Carbon monoxide poisoning of proton-exchange membrane fuel cells. Energy Conversion Engineering Conference, 1997.

Sammes, N., 2006. Fuel Cell Technology. London, UK: Springer.

Savage, L., M., 2008. Testing Methanol-Based Fuel Cells Using FTIR Spectroscopy. *Photonics spectra* 42, 31-32(2008)

Schmidt-Rour, K. and Chen, Q., 2008. Parallel cylindrical water nanochannels in Nafion fuel-cell membranes. *Nature Materials*, 7, 75-83(2008)

Sedighizaheh, M. and Rezazadeh, A. 2007. Comparison between Batteries and Fuel Cells for Photovoltaic System Backup. *Proceedings of World Academy of Science, Engineering and Technology* 26, 772-776(2007)

Shukla, A., Neergat, M., Bera, P., Jayaram, V. and Hegde, M., S., 2001. An XPS study on binary and ternary alloys of transition metals with platinized carbon and its bearing upon oxygen electroreduction in direct methanol fuel cells. *Journal of Electroanalytical Chemistry,* 504, 111-119(2001)

Song, S., Q., Zhou, W., J., Li, W., Z., Sun, G., Xin, S., Kontou, S. and Tsiakaras, P, 2004. Direct methanol fuel cells: methanol crossover and its influence on single DMFC performance. *Ionics,* 10, 458-462(2004)

Suarez, M., 2013. The effect of membrane thickness on the performance of PBI-based high-temperature Direct Methanol Fuel Cells. Worcester Polytechnic institute.

U.S. Energy Information Administration: available from http://www.eia.gov/

Vielstich, W., Lamm, A. and Gasteiger, H., A., 2009. Handbook of Fuel Cells- Fundamentals, Technology and Applications. Hoboken, New Jersey: John Wiley & Sons, Inc.

Voth, G., A., 2006. Computer simulation of Proton solvation and transport in aqueous and biomolecular systems. *American Chemical Society*, 39, 143-150(2006).

Wang, J., T., Wainright, J., S., Savinell, R., F. and LItt, M., 1996. A direct methanol fuel cell using acid-doping polybenzimidazole as polymer electrolyte. *Journal of Applied Electrochemistry,* 26, 751(1996)

Wang, J., T., Wasmus, S. and Savinell, R., F., 1996. Real-Time Mass Spectrometric Study of the Methanol Crossover in a Direct Methanol Fuel Cell. *Journal of Elctrochem Society,* 143, 1233-1239(1996).

Wasmus, S., and Kuver, A., 1998. Methanol oxidation and direct methanol fuel cells: a selective review. *Electroanalytical Chemistry,* 461, 14-31(1998)

Waszczuk, P., Wieckowski, A., Zelenay, P., Gottesfeld, S., Coutanceau, C., Leger, J., M. and Lamy, C., 2001. Adsorption of CO poison on fuel cell nanoparticle electrodes from methanol solutions: a radioactive labeling study. *Journal of Electroanalytical Chemistry*, 511, 55-64(2001)

Wu, J., 2013. Polyimide polybenzimidazole intermediate transfer members. US20130052375 A1

Yan Q, Liu Q, and Wu J., 2008. Modeling CO poisoning and O2 bleeding in PEM Fuel Cells. 214th ECS Meeting, Honolulu, HI. 2008.

Zhang, J. and Datta, R., 2002. Sustained potential oscillations in proton exchange membrane fuel cells with PtRu as anode catalyst. *Journal of the Electrochemical Society*, 149, A1423-A1431 (2002).

Zhou, X., Chen, Z., Delgado, F., Brenner, D. and Srivastava, R., 2007. Atomistic simulation of conduction and diffusion process in Nafion polymer electrolyte and experimental validation. *Journal of The Electrochemical Society*, 154, B82-B87 (2007).

Appendix A: Acronym List

°C	Degrees Celsius
BASF	Badische Anilin-und Soda-Fabrik
cm^2	Centimeter Squared
mA	milliampere
V	volt
CO	Carbon Monoxide
CO_2	Carbon Dioxide
DFMC	Direct Methanol Fuel Cell
e^-	Electron
GDL	Gas Diffusion Layer
MEA	Membrane Electrode Assembly
mW	milliwatts
OCV	open Circle Voltage
T	temperature
PBI	Polybenzimidazole
Pt	Platinum

Ru	Ruthenium
mL	Milliliter
min	Minute
PEM	Proton exchange membrane

Appendix B: Instructions for fuel cell test station

Syringe Pump

Figure 57 Syringe Pump

The syringe pump was a Teledyne Isco D-series syringe pumps, which can control flow and pressure at a good operating range. This syringe pump can be used in a wide variety of fluids, such as organic liquids, heated fluids, liquefied gases and corrosive solutions.

The followings are the method to use this syringe pump:

1. Turn on power to the pump by activating the power switch.
2. Remove tubing connection to furnace and put it in the collection vessel.

3. Press “A”, than change the flow rate to the numerical value desired, and press “enter” to ensure.
4. Press “Run” to pump methanol form the pump.
5. When the pump is empty remove the tubing from the collection vessel and place it into methanol container.
6. Press “Refill” button to refill the pump.
7. When the pump is full, wait a few minutes for the pressure in the pump to 16 psi.
8. Turn the pump to “Run” mode until some liquid flows into the vessel, stop the pump and connect the line to furnace.
9. Press “Run” to pump methanol into fuel cell system.

Hints for use

1. Check the flowrate setting before press “Run”, because the refilling flowrate is much larger than the running flowrate.
2. After filling the pump, running at a higher flowrate will ensure that the line has no air left in it.
3. Keep the pressure in the pump below 30 psi for the health of the pump.
4. When complete one group of test, the pump should be emptied and refill with deionized water.
5. If change methanol water mix solution to another concentration, the pump should be also emptied and refill with deionized water.

Temperature Controller

Figure 58 Temperature control boxes

The three temperature were built to control the temperature of furnace, the fuel cell and the methanol feed line, which are shown in Figure 58. The temperature controllers that were used are CN9000A series autotune temperature controller from Omega. The model of CN9000A is shown in Figure 59, which shows how it works.

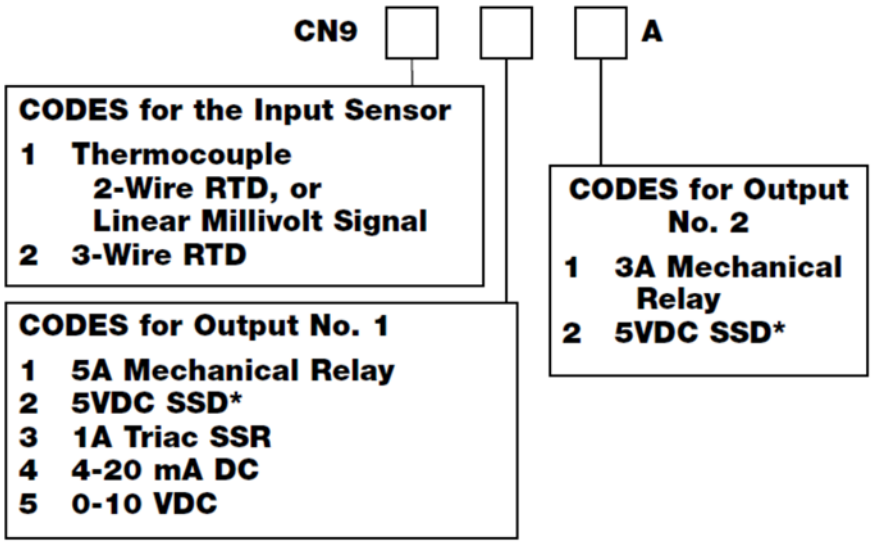

Figure 59 CN9000A model number information (C9000A series autotune temperature controller user's guide)

In the fuel cell test station, the three temperature controllers are connected with heating tapes throughout the apparatus, and they also are connected with thermocoulpes, which are located in the furnace, fuel cell and methanol feed line to feedback the temperature. Heating tapes are used to heat the various parts of the apparatus. Cooling is be done by free convection with the atmosphere.

Load box

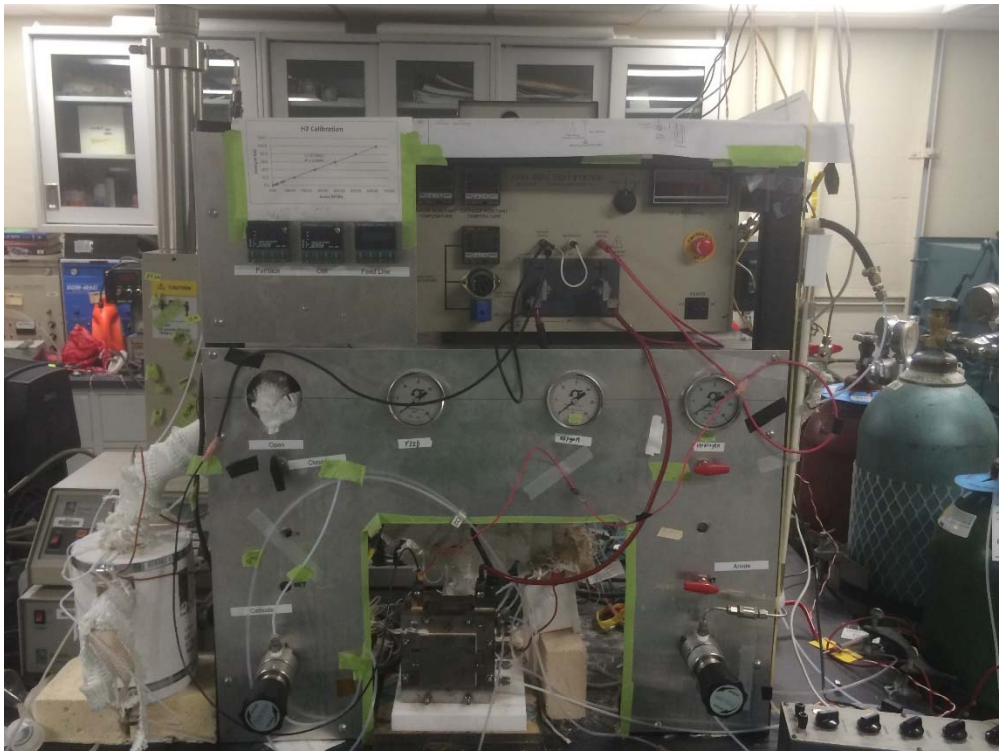

Figure 60 Loading box

Figure 60 is shown that the loading box was used in the fuel cell test station. It is 890B fuel cell test system. The loading box is connected with computer, which can help control the voltage, current and record test data. Figure 61 is the setup fuel table.

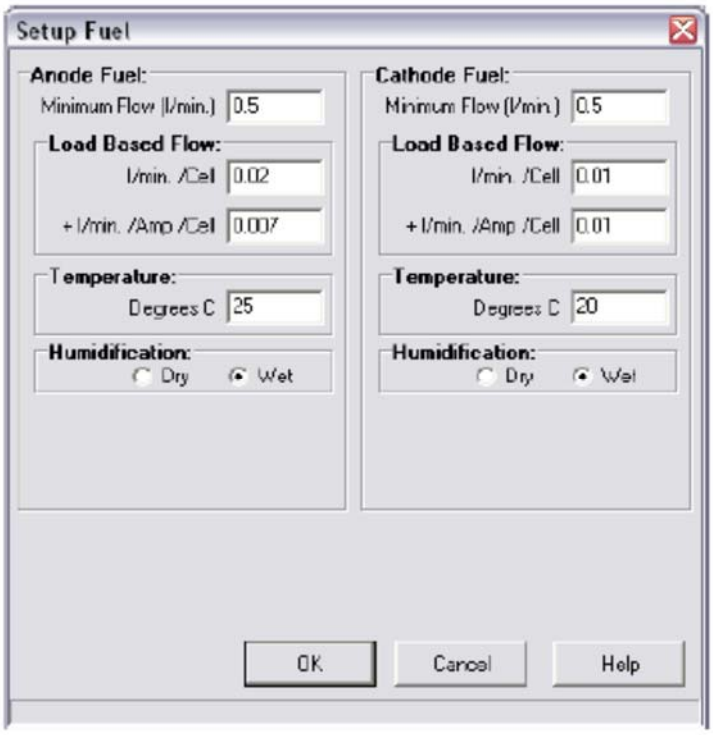

Figure 61 setup fuel table

By this loading box, I can input the voltage and current density desired and get the output data to record.

Methanol feed

Starting feed

1. Check if there is enough methanol in pump.
2. If need, follow the direction to refill the pump.
3. Adjust temperature for methanol feed line.
4. Check the temperature of methanol to ensure that there is no liquid mixed with the vapor methanol.
5. Switch the methanol feed line to fuel cell.

6. During the test, if methanol in the pump is not enough, refill the pump and inlet nitrogen on both sides of fuel cell.

Stopping feed

1. Stop the syringe pump.
2. Return temperature settings to 0.
3. Inlet nitrogen on both sides of fuel cell to protect PBI MEA.
4. Use deionized water to replace methanol in the pump.

Hydrogen feed

Starting feed

1. Open globe valve on the hydrogen tank.
2. Adjust pressure regulator to 2 psi.
3. Open the check valve.

Stopping feed

1. Close globe valve on the hydrogen tank.
2. Adjust pressure regulator to no pressure.
3. Close the check valve.

Oxygen feed

Starting feed

1. Open globe valve on the oxygen tank.
2. Adjust pressure regular to 2 psi.

3. Open needle valve.
4. Open check valve.

Stopping feed

1. Close globe valve on the oxygen tank.
2. Adjust pressure regular to 0.
3. Close needle valve.
4. Close check valve.

Nitrogen feed

Starting feed

1. After every test, remove methanol feed line and oxygen feed line, switch to nitrogen feed line on both sides of fuel cell.
2. Open globe valve on the nitrogen tank.
3. Adjust pressure regulator to desired pressure.
4. Open the check valve.

Stopping feed

1. Close the globe valve on nitrogen tank.
2. Adjust pressure regulator to 0.
3. Close check valve.

Appendix C: support data

There is an example of the experiment test data.

5mol/L methanol current scan

160C			170C			180C		
Current density/ mA/cm2	volt/V	Power density/ mW/cm 2	Current density/ mA/cm2	volt/V	Power density/ mW/cm 2	Current density/ mA/cm2	Volt/V	Power density/ mW/cm 2
0	0.5702 4	0	0	0.5932 5	0	0	0.571 15	0
2.1703	0.5549 8	1.2044	2.1707	0.5879 7	1.2763	0.17524	0.612 96	0.10742
4.4461	0.4779 5	2.125	4.4447	0.5180 5	2.3026	0.17294	0.627 92	0.10859
6.6667	0.4314 7	2.8765	6.6671	0.4597 6	3.0653	0.17294	0.638 9	0.11049
8.889	0.4020 5	3.5738	8.889	0.4352 2	3.8687	1.5057	0.638 14	0.96086
11.111	0.3896 9	4.3298	11.111	0.4263 7	4.7376	0.92925	0.636 77	0.59172
13.333	0.3732 7	4.9769	13.333	0.4031 5	5.3751	1.2913	0.635 55	0.82067
15.556	0.3564 3	5.5446	15.557	0.3713 2	5.7766	1.5265	0.628 53	0.95943
17.778	0.3400 7	6.0456	17.779	0.3733	6.6368	1.7409	0.623 65	1.0857
19.999	0.3233 4	6.4666	20	0.3615 8	7.2318	1.9692	0.622 58	1.226
22.222	0.3198 6	7.1081	22.221	0.3285	7.2998	2.1929	0.619 83	1.3592
24.446	0.3036 3	7.4224	24.446	0.3256 9	7.9619	2.4488	0.616 78	1.5104
26.667	0.2885 8	7.6955	26.667	0.3186 4	8.4973	2.6656	0.611 9	1.631
28.889	0.2814 1	8.1298	28.889	0.3054	8.8225	2.8454	0.607 17	1.7276
31.112	0.2690 2	8.3697	31.111	0.2936 5	9.1357	3.1267	0.599 23	1.8736

33.334	0.26399	8.7996	33.334	0.27976	9.3257	3.2974	0.59771	1.9708
35.555	0.25465	9.054	35.555	0.27226	9.68	3.5579	0.59191	2.106
37.777	0.23588	8.9107	37.774	0.26896	10.16	3.7977	0.58718	2.2299
39.999	0.22864	9.1457	40	0.24818	9.927	3.9983	0.58199	2.327
42.223	0.21946	9.2661	42.226	0.24561	10.371	4.2197	0.57695	2.4346
44.445	0.21479	9.5463	44.443	0.24107	10.714	4.4572	0.56978	2.5396
46.667	0.20591	9.6092	46.667	0.2226	10.388	4.6716	0.56185	2.6247
48.89	0.19413	9.4909	48.89	0.20728	10.134	4.8884	0.55315	2.704
51.11	0.18888	9.6537	51.11	0.20844	10.654	5.1005	0.54506	2.7801
53.333	0.17734	9.4582	53.334	0.19691	10.502	5.3426	0.53774	2.8729
55.556	0.17057	9.476	55.557	0.18589	10.327	5.5548	0.53423	2.9675
57.777	0.16358	9.4511	57.779	0.17872	10.326	5.7807	0.5269	3.0459
59.999	0.15363	9.2177	59.999	0.17356	10.413	6.0067	0.51866	3.1155
62.223	0.14194	8.832	62.221	0.15873	9.8762	6.2142	0.5118	3.1804
64.446	0.13779	8.8801	64.446	0.15412	9.9323	6.4402	0.50493	3.2519
66.667	0.12854	8.5696	66.666	0.14536	9.6906	6.6662	0.49898	3.3263
68.889	0.12116	8.3465	68.888	0.13627	9.387	6.8806	0.50295	3.4606
71.111	0.11646	8.2815	71.111	0.1297	9.2234	7.1066	0.50401	3.5818
73.329	0.1062	7.7879	73.332	0.1178	8.6386	7.3349	0.50661	3.7159
75.559	0.093783	7.0862	75.558	0.10605	8.0131	7.5424	0.50691	3.8233
77.779	0.087497	6.8054	77.774	0.1059	8.2362	7.7707	0.50478	3.9225

79.993	0.083224	6.6574	79.991	0.089328	7.1454	7.9921	0.50081	4.0025
82.184	0.0759	6.2377	82.247	0.082644	6.7972	8.2111	0.50157	4.1185
80.02	0.083377	6.6718	84.493	0.080264	6.7817	8.4371	0.50218	4.2369
77.776	0.0918	7.1398	85.306	0.073397	6.2612	8.6538	0.49516	4.2851
75.552	0.092624	6.9979	84.457	0.073275	6.1886	8.8821	0.48723	4.3276
73.334	0.10337	7.5802	81.936	0.084933	6.9591	9.1012	0.4799	4.3677
71.111	0.11301	8.0363	80.002	0.097232	7.7788	9.3317	0.47807	4.4613
68.887	0.12326	8.4913	77.764	0.098666	7.6727	9.5508	0.47548	4.5412
66.667	0.12937	8.6245	75.563	0.10218	7.7208	9.7699	0.4651	4.544
64.445	0.13675	8.8131	73.332	0.12244	8.9788	9.9912	0.45854	4.5814
62.222	0.14664	9.1243	71.109	0.1305	9.2795	10.215	0.46098	4.7089
60.002	0.14997	8.9983	68.888	0.12812	8.8256	10.436	0.46312	4.8332
57.776	0.16163	9.3381	66.667	0.14402	9.6011	10.665	0.46434	4.952
55.556	0.16837	9.354	64.444	0.15589	10.046	10.879	0.46205	5.0266
53.332	0.18015	9.6079	62.222	0.16163	10.057	11.103	0.45778	5.0825
51.112	0.18949	9.6852	60.001	0.16755	10.053	11.326	0.45137	5.1123
48.891	0.19309	9.4404	57.779	0.18143	10.483	11.543	0.45106	5.2066
46.667	0.2002	9.3428	55.558	0.19663	10.924	11.767	0.45259	5.3255
44.444	0.21213	9.428	53.333	0.19633	10.471	11.988	0.45076	5.4037
42.223	0.22269	9.4027	51.112	0.20521	10.489	12.221	0.44832	5.4789
39.998	0.23344	9.337	48.89	0.21894	10.704	12.412	0.44801	5.5609

37.778	0.24204	9.1439	46.666	0.22803	10.641	12.664	0.4445	5.629
35.554	0.24775	8.8084	44.444	0.23081	10.258	12.876	0.44221	5.6939
33.334	0.25904	8.6348	42.221	0.24726	10.44	13.109	0.44053	5.7748
31.111	0.27207	8.4644	39.999	0.26148	10.459	13.314	0.44008	5.8592
28.89	0.28355	8.1917	37.779	0.26753	10.107	13.542	0.43855	5.939
26.667	0.29093	7.7583	35.555	0.26322	9.3588	13.764	0.4358	5.9982
24.444	0.30335	7.4153	33.334	0.29112	9.7041	13.994	0.42879	6.0005
22.222	0.31434	6.9854	31.111	0.30659	9.5384	14.216	0.4268	6.0672
20	0.32838	6.5677	28.888	0.29789	8.6054	14.425	0.42756	6.1678
17.779	0.34318	6.1012	26.667	0.31504	8.4013	14.658	0.4265	6.2517
15.556	0.35597	5.5375	24.444	0.33421	8.1695	14.847	0.43504	6.4592
13.333	0.37648	5.0195	22.223	0.34767	7.7261	15.096	0.43062	6.5007
11.112	0.38774	4.3085	20.001	0.34394	6.8792	15.325	0.42482	6.5102
8.8886	0.40809	3.6274	17.778	0.38081	6.7699	15.548	0.4178	6.4961
6.6671	0.43577	2.9054	15.556	0.39442	6.1357	15.747	0.42497	6.6918
4.4452	0.46931	2.0862	13.333	0.38853	5.1804	15.998	0.42985	6.8768
2.2214	0.52406	1.1642	11.11	0.41884	4.6533	16.208	0.43153	6.9942
0	0.58629	0	8.889	0.45784	4.0697	16.427	0.4268	7.011
			6.6662	0.46144	3.076	16.655	0.42528	7.083
			4.4434	0.50383	2.2387	16.879	0.41841	7.0622
			2.2214	0.5642	1.2533	17.096	0.41337	7.0668

			0	0.60949	0	17.328	0.4088	7.0838